A STUDY ON EFFECT OF GEO-REINFORCEMENT IN PERFORMANCE IMPROVEMENT OF FLEXIBLE PAVEMENT

Submitted for the Partial Fulfillment of Degree of Master in Engineering (M.E.) in Civil Engineering

BY

ANAL KRISHNA MALAKAR

Class Roll No. **-002010402014**

University Registration No.**-153970 of 2020-21**

Under the Guidance of

Dr. Pritam Aitch
Associate Professor
Civil Engineering Department,
Jadavpur University

Dr. Arghadeep Biswas
Assistant Professor
Civil Engineering Department,
Jadavpur University

Civil Engineering Department
Jadavpur University
Kolkata 700032
November, 2022

JADAVPUR UNIVERSITY
FACULTY OF ENGINEERING AND TECHNOLOGY
DEPARTMENT OF CIVIL ENGINEERING

DECLARATION OF ORIGINALITY AND COMPLIANCE OF ACADEMIC ETHICS

I, ANAL KRISHNA MALAKAR having Class Roll No. – 002010402014,Exam Roll no-M4CIV22014(B) and University Regd. No. – 153970 of 2020-21 do hereby declare that this thesis titled "**A Study on effect of geo-reinforcement in performance improvement of flexible pavement**" contains literature survey and original research work done by the undersigned candidate, as part of his Master of Engineering in Civil Engineering with specialization in Soil Mechanics & Foundation Engineering studies.

All the information in this thesis have been obtained and presented in accordance with existing academic rules and ethical conduct. I declare that, as required by these rules and conduct, I have fully cited and referred all materials and results that are not original to this work.

Signature of Candidate:

Date:

Certified by Supervisor(s):
(Signature with date, seal)

1. 2.

JADAVPUR UNIVERSITY

Faculty of Engineering and Technology
Department of Civil Engineering

CERTIFICATE OF RECOMMENDATION

*we do hereby recommend that the thesis prepared under my supervision by Sri Anal Krishna Malakar (Roll no: 002010402014) entitled "**A STUDY ON EFFECT OF GEO-REINFORCEMENT IN PERFORMANCE IMPROVEMENT OF FLEXIBLE PAVEMENT**" be accepted in partial fulfilment of the requirements for the Degree of Master of Civil Engineering with specialization in Soil Mechanics & Foundation Engineering from Jadavpur University, Kolkata-700032.*

Thesis Supervisor(s)

…….	……
Dr. Pritam Aitch	*Dr. Arghadeep Biswas*
Associate Professor	*Assistant Professor*
Department of Civil Engineering	*Department of Civil Engineering*
JADAVPUR UNIVERSITY	*JADAVPUR UNIVERSITY*

Countersigned by

……..	…….
Head of Department	*DEAN*
Civil Engineering Department	*Faculty of Engineering and Technology*
JADAVPUR UNIVERSITY	*JADAVPUR UNIVERSITY*
Kolkata-700032	*Kolkata- 700032*

JADAVPUR UNIVERSITY
FACULTY OF ENGINEERING AND TECHNOLOGY
DEPARTMENT OF CIVIL ENGINEERING

CERTIFICATE OF APPROVAL

The foregoing thesis is hereby approved as a creditable study of an Engineering subject carried out and presented in a manner satisfactory to warrant its acceptance as a pre- requisite to the degree for which it has been submitted. It is understood that by this approval the undersigned do not necessarily endorse or approve any statement made, opinion expressed or conclusion drawn therein, but approve this thesis only for the purpose for which it is submitted.

Board of Thesis Examiners:

1……

2……

3……

ACKNOWLEDGEMENT

I Would like to express my wholeheartedly and deep gratitude to Prof. Dr. Pritam Aitch, Prof. Dr. Arghadeep Biswas Department of Civil Engineering, Jadavpur University, for his valuable guidance, constant support and encouragement throughout my thesis work. This has been a precious opportunity for me not only to gain knowledge and skill but also to learn much more about approaches, attitudes towards work and interpersonal relationship.

I am sincerely thankful and indebted to Prof. Dr.Partha Bhattacharya, Prof. Dr.Ramendu Bikas Sahu, Prof. Dr.Gupinath Bhandari, Prof. Dr.Sibapriya Mukherjee of Civil Engineering Department for their constant encouragement and continuous valuable suggestions throughout my thesis work. I would also like to express my gratefulness to Prof. Dr.Sumit Kumar Biswas, Prof. Dr.Narayan Roy, Prof. Dr.Obaidur Rahaman and Staffs of Civil Engineering Department, Jadavpur University for extending all facilities to carry out the present study.

Last but not the least, I express my sincere gratitude to all of my friends, seniors and my parents for their co-operation during the preparation on my thesis. It is due to their regular encouragement and enlightening discussions for which thesis this could be brought to current shape.

ANAL KRISHNA MALAKAR
Class Roll No:-002010402014
MCE Student (Specialization:
Soil Mechanics & Foundation Engineering),
Department of Civil Engineering,
Jadavpur University, Kolkata 700032

Signature and date ……

Symbols and Abbreviations

AASHTO	American Association of State Highway and Transportation Officials
ASTM	American Society of Testing and Materials
BC	Bituminous Concrete
BM	Bituminous Macadam
CBR	California Bearing Ratio
CPVD	Commercial Vehicles per Day
COV	Coefficient of Variation
DBM	Dense Bituminous Macadam
F_R	Reliability Design Factor
GPR	Ground Penetrating Radar
IRC	Indian Road Congress
M_R	Resilient Modulus
MSA	Million Standard Axles
MORTH	Ministry of Road Transport and Highways
N_f	Cumulative Number of Repetitions for Fatigue Failure
N_t	Actual Number of ESALs, a structure can withstand
N_T	Actual Number of ESALs that will be applied for the design period
SAMI	Stress Absorbing Membrane Interlayer
RAP	Reclaimed Asphalt Pavement
V_a	Volume of Air Voids
V_b	Volume of Bitumen
VDF	Vehicle Damage Factor
WMM	Wet Mix Macadam
w_T	Predicted ESALs that will be applied to the pavement for the design period
W_t	Predicted ESALs that a structure can withstand
$Z_{\frac{\alpha}{2}}$	Associated z-statistics from standard normal table
ϵ_a	Axial Strain
ϵ_t	Horizontal Tensile Strain
ϵ_V	Vertical Subgrade Strain
ϑ	Poisson's Ratio

Table of Contents

ABSTRACT

In this study, a numerical analysis is carried out for the evaluation of both unreinforced and reinforced flexible pavements based on the California Bearing Ratio (CBR) values of subgrade and traffic loads using the IITPAVE. The IITPAVE is a robust mechanistic-empirical method-based software developed by the Department of Civil Engineering, IIT Kharagpur and appreciated and incorporated by the Indian Road Congress in their standard (IRC-37). The behaviour of base, sub-base, and subgrade soil has been simulated using a linear elastic model. In the recent past, geosynthetics have been found to be a cost-effective alternative to improve weak subgrades in adverse locations. Therefore, in this study, the influence of introducing a geosynthetic material, namely the geogrid, in the base layer of flexible pavements is investigated. It is noticed that the inclusion of geogrid in the base layer of flexible pavement has reduced the base thickness by 87% as compared to the corresponding unreinforced section. This study was conducted on the reinforced and unreinforced pavement sections constructed on a subgrade having a moderate California bearing ratio (CBR) value of 5% and traffic value of 100 MSA. In this study, the flexible pavement has been designed for both fatigue and rutting life of 100MSA at 90% and 80% levels of reliability. The critical strain value for both fatigue and rutting life are analyzed by the IITPAVE and are found to be less than the prescribed allowable strain values as computed by IRC: 37-2012. The inclusion of geogrid in the pavement layer helps in improving the reduction of vertical compressive strain, and reduction in surface deformation by an amount of 57% and also provides an economical solution saving the natural resources used in pavement constructions. It is found that reinforced pavement costs approximately 40% cheaper than unreinforced pavement.

Chapter 1

INTRODUCTION

Indian Road Network of approximately 60 lakh km is the 2nd largest in the world. Among that, the great majority of pavements are flexible type. The bitumen layer, surface course, aggregate layers, and subgrade soil are typically included in the design of flexible pavements. The type of sub-grade, sub-base, and base course layers have a significant impact on the quality and lifespan of the pavement. Constant increases in traffic frequency and axle loads place great demands on the existing road network. The stresses created between layers quickly lead to the development of cracks, and any small differential settlements at the subgrade may cause further settlement of top layers. In the last few decades, geosynthetics have gained popularity in pavement construction. Since geogrid can confine the infill material, in addition to the reinforcement functions provided by traditional geosynthetics, the use of geogrid in pavement layers is more compared to others. Their use has been proven to be cost-effective in improving the bearing capacity and settlement performance of earth structures. The most common types of geosynthetics include Geogrids, Geotextiles, Geomembranes, Geosynthetic, Geonets etc.

1.1 Types of Pavements

Mostly, there are two categories of pavement, depending on the structural composition.

Rigid pavement:

Cement concrete or slabs of reinforced concrete are used to create rigid pavement. The foundation of rigid pavement design is a structural slab of cement concrete that is strong enough to withstand the loads carried on by traffic. The rigid pavement's rigidity and high elastic modulus help it disperse the weight over a significant amount of soil. Small differences in subgrade strength have little impact on a rigid pavement's structural strength. The main consideration in the design of a rigid pavement is the flexural strength of concrete, not the strength of the subgrade. This characteristic of pavement allows the concrete slab to bridge over localized failures and regions of insufficient subgrade support when the subgrade flexes beneath the rigid pavement. A typical cross-section of a rigid pavement is shown in Figure 1.1 [8]

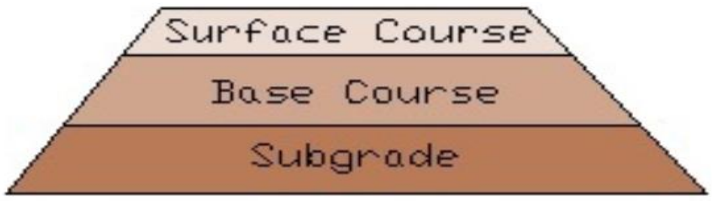

Figure 1.1: Typical cross-section of a rigid pavement [8]

Flexible pavement:

Pavements that are flexible in their structural activities under loads are those that have low flexural strength. Based on the load-distributing properties of the component layers, flexible pavement is designed. Flexible pavements do have some flexural strength, although it is very little. Soil subgrade, sub-base, base course, and surface course are the four parts that make up a conventional flexible pavement. A typical cross-section of flexible pavement is given in Figure 1.2 [9]

Figure 1.2: Typical cross-section of a flexible pavement [9]

1.3 Geosynthetics

Geosynthetic is defined as a planar product manufactured from a polymeric material that is used with soil, rock, or other geotechnical-related material as an integral part of civil engineering projects. The polymeric nature of the products makes them suitable for use on the ground where high levels of durability are required. The most common types of geosynthetics are discussed below:

1.3.1 Categories of Geosynthetics

Geotextile	Geogrid
Geomembrane	Geo-composite
Geonets	Geofoams

1.Geotextile

Fabrics made from synthetic materials including polypropylene, polyamide, polyethene, and glass fibres are called geotextiles and are porous or permeable. Geotextiles are a fundamental component of manufactured goods that are used with soil. Modern geotextiles' resistance to biological and chemical deterioration makes them suitable for both building and maintaining roads. They can have a thickness of 0.125 to 7.5 mm. The geotextile sheets' permeabilities, which range from fine sand to coarse gravel, are comparable. Geotextiles are typically created as woven or non-woven fabrics.

Non-woven Geotextiles and woven Geotextiles

Short staple fibres can be used to create non-woven geosynthetics in sheets with an orientated or random pattern, or continuous filament yarn can be used. Thermal, mechanical, or chemical methods are used to join these fibres together. The normal thickness of thermally bonded non-woven geotextiles is between 0.5 and 1 mm, and they have a large aperture size. Mechanically bonded non-woven with a thickness of 2 to 5 mm. Due to their low tensile strength, non-woven geotextiles have a low load-carrying capability. Non-woven fabric is more stretchable than woven. Non-woven have the to let water flow along the plane of the geotextile.

The woven geotextile sheet is made up of two sets of parallel thread or yarns. The yarns running along its length are called the warp and one perpendicular to it is known as a waft. Low to medium-strength woven-geotextile are generally manufactured from polypropylene and is in the form of monofilament, multifilament, extruded tape etc. Multifilament or monofilament has a higher permeability than extruded tape. In general, woven geotextiles are less likely to stretch than non-woven ones and do not allow water to flow as freely. Geotextiles are shown in Figure.1.3 [10]

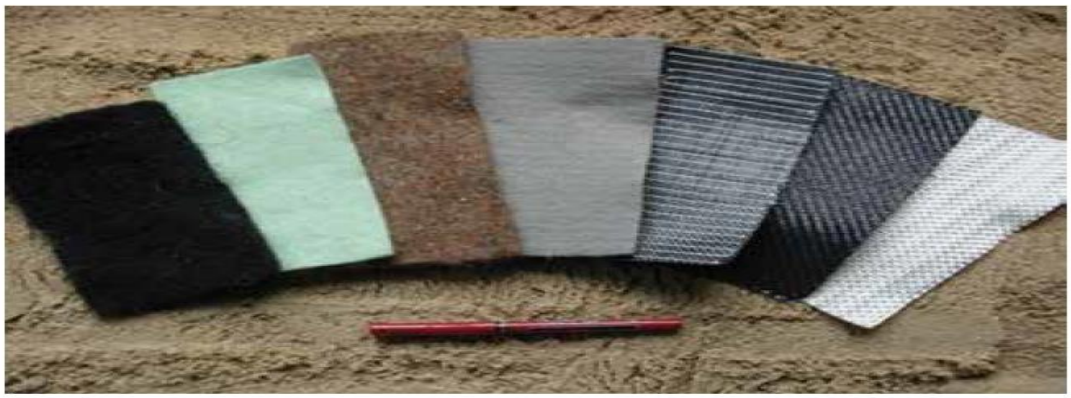

Figure 1.3: Geotextile [10]

2. Geogrid:

Geogrid is a major type of geosynthetics which has an open mesh grid structure. It can be used for soil reinforcement, separation, drainage and filtration in roads, airfields, railroads, embankments, earth retaining structures, reservoirs, canals, dams, and coastal protection. Uniaxial, biaxial, and triaxial geogrids are three common types of geogrid. Recently, geogrids have been widely used for soil reinforcement of paved and unpaved roads where weak soil. Geogrids are geosynthetics formed with open apertures and grid-like configurations of orthogonal or non-orthogonal ribs. Koerner (1998) defines a geogrid as a "geosynthetic material consisting of connected parallel sets of tensile ribs with apertures of sufficient size to allow for strike-through of the surrounding soil, stone, or other geotechnical material." Extruding and drawing sheets of Polyethylene (PE) or Polypropylene (PP) plastic in one or two directions or weaving and knitting Polyester (PET) ribs are methods used to produce geogrids. Geogrids are designed mainly to satisfy the reinforcement function. The ribs of a geogrid are defined as either longitudinal or transverse. A typical geogrid is shown in Figure 1.4 [10]

Figure 1.4: Geogrid [10]

3. Geomembrane:

A geomembrane is a synthetic membrane with a very low permeability that is made from thermoplastics like HDPE, LDPE, and PVC or as multi-layered bitumen geo-composites. Geomembranes are produced either extruded sheet polymer or composite. This sheet is created using either a horizontal flat die or a vertically oriented circular die to create a flat, wide sheet that is advanced on a conveyor belt or a hollow, blown-film tube that is pushed and deflated by nip rollers that are located far above the die. The geomembrane's thickness ranges from 10 to 15 mm. Bitumen-reinforced membranes can range in width from 4 to 5 mm and thickness from 1.5 to 6 mm. The geomembrane is shown in Figure 1.5 [10]

Figure 1.5: Geomembrane [10].

4. Geo-composite:

A geo-composite is a unit that is manufactured in a factory using a combination of geotextiles, geogrids, geonets, and/or geomembranes. Drainage geo-composite is the name given to the most popular geo-composite design. Drainage geo-composites are composed of a geotextile filter surrounding either a geonet (blanket drain), a thick preformed core (panel or edge drain), or a thin preformed core (wick drain). Geo-composite is shown in Figure 1.6 [10].

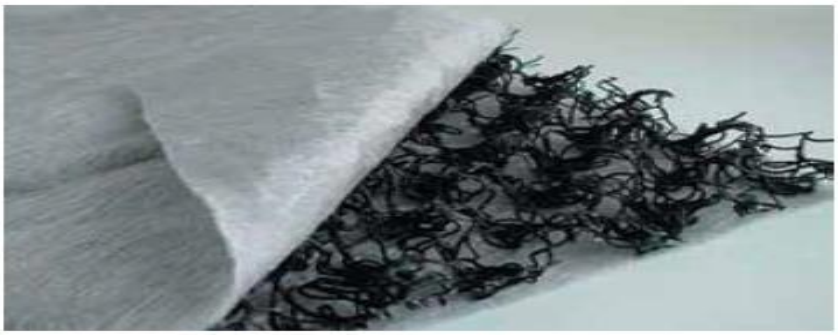

Figure 1.6: Geocomposite [10].

5. Geonet:

Geonets are made of two sets of spherical polymer strands that cross at an angle that is always the same, resulting in an extremely open material with significant diamond- or rectangle-shaped perforations. Polyethene is used to create almost all geonets. The strands' and apertures' sizes are 2 mm and 7 mm, respectively. To increase the elastic modulus, the nets are occasionally softly stretched during the manufacturing process. The geonets' strengths range from 2 to 10 KN/m. Geonet is shown in Figure 1.7 [10].

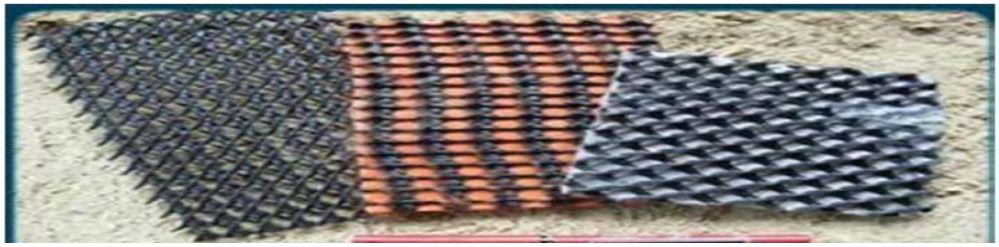

Figure 1.7: Geonet [10].

6. Geofoams:

A lightweight, thermally insulating substance called geofoam is produced as huge blocks that are stacked and buried in pavement or earth. Polystyrene is the most prevalent form of polymer utilised in the production of geofoam products.

Geofoams are commonly used for a wide range of purposes, such as under highways, airport pavements, and railway track systems that are vulnerable to extreme freeze-thaw conditions. Sometimes it is used beneath on-grade storage tanks containing cold liquids. Geofoams are shown in Figure 1.8 [11].

Figure 1.8: Geofoams [11].

1.4.2 Performance benefits of geosynthetic reinforcement in the flexible pavement:

Geosynthetics provide a long-term and economical solution to a wide variety of engineering applications, such as base reinforcement and soil stabilization for pavement foundations, mechanical stabilization for earth structures (i.e., steepened slopes, retaining walls, and embankments), erosion and drainage control, landfill and waste-containment projects, root barrier, water retention, capillary mat drainage composites, and filtration.

Many studies have been carried out to examine the mechanisms of geosynthetic reinforcement. These mechanisms include lateral restraint, enhanced bearing capacity, tension membrane effects, and separation as described as follows.

I. Lateral Confinement: The unbound base course layer spreads laterally in response to loads placed on the pavement. As the material falls from the applied load, tensile lateral strains are initiated in the base layer. This site movement is reduced and constrained by the geosynthetic, which limits the base aggregates. The

term lateral confinement consists of several factors of reinforcement as well (i) confining the side movement of base aggregate, (ii) increasing the stiffness of the base aggregate layer, (iii) reducing the shear stress in the subgrade soil layer, and (iv) developing the vertical stress distribution on the top of the subgrade. This mechanism of the reinforced base is illustrated in Figure 1.9(a).[10]

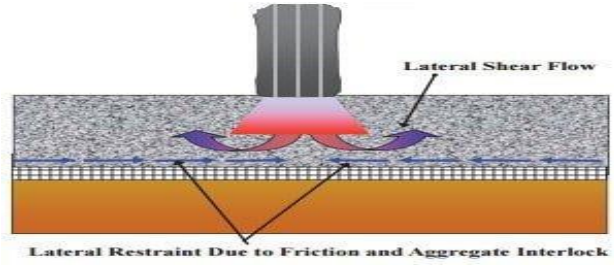

Figure 1.9(a) lateral resistance due to friction [10].

II. Mechanism for improved bearing capacity: By shifting the failure envelope from the comparatively weak subgrade to the relatively strong base layer of the pavement system, the bearing capacity is improved, as illustrated in Fig.1.9(b) [10]. As result bearing failure of subgrade from punching failure without reinforcement is limited when reinforcement is used.

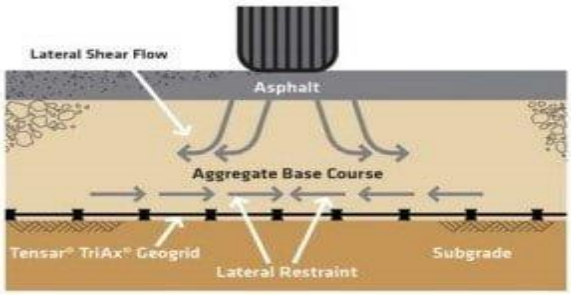

Figure 1.9(b): Mechanism for improved bearing capacity [10].

III. Tension Membrane Effect: The tension membrane effect is caused by vertical deformation, which causes the tensioned geogrid layer to take on a

concave shape, as illustrated in Fig.1.9(c) [10]. It can reduce the vertical stress acting on the subgrade. Typically, a greater deformation is required for the mobilization of resistance of the tensile membrane as the stiffness of the geogrid declines, to establish the membrane effect and increase the bearing capacity of the subgrade layer, significant rutting depth and high stiffness of the geosynthetics should be allowed.

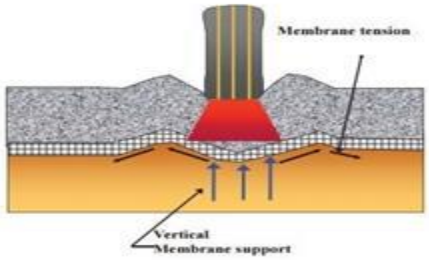

Figure 1.9(c): Tension membrane effect [10]

IV. Separation: Separation is one of the most important geo-reinforcement mechanisms in pavements. Due to the traffic loads, fine particles from the subgrade moving into the aggregate base layer leads to a fall in their desired qualities. Mixing at the base course/subgrade zone reduces the effective base thickness/layer modulus, which probably causes the pavement system to collapse structurally. Between the subgrade and base interface, a geogrid layer serves as a separator layer that might prevent this mixture.Fig.1.9 (d) [13] demonstrates the separation effect.

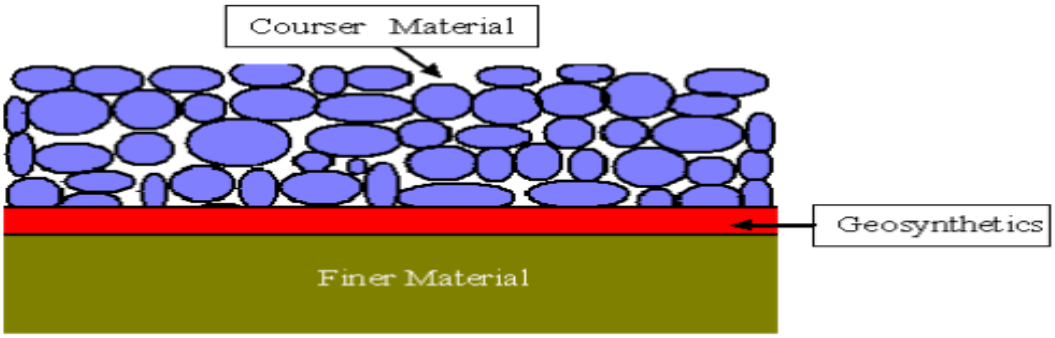

Figure 1.9(d): Mechanism of separation of geosynthetics in soil-aggregate layer [13].

1.5 Objectives of the Study

This study "A study on the effect of geosynthetic-reinforcement on the performance improvement of flexible pavement" is having the following objectives.

- The introduction of geosynthetics influences the pavement layer thickness and the use of geosynthetics enhance the performance of the flexible pavement.
- To investigate the deformation behaviour of geosynthetic-reinforced pavement.
- Reinforce the pavement structure to save natural resources, optimize the pavement performance, and cost efficiency of reinforced pavements.

1.6 Scope of the Work:

To achieve the above mention objective a Mechanistic-Empirical study is carried out through the IITPAVE software, where stress, strain, and deformation values

are measured with change in thickness, subgrade, and sub-base modulus. The major scopes of our project paper are as follows:

- A literature review was conducted to investigate issues in performance-based pavement design and characterization of the relevant design variables.
- For this project, it is important to find out the statistical variation pattern of various factors like layer thickness, Resilient Modulus and property of reinforcement (i.e. geogrid).
- This allowed for an in-depth analysis regarding the relative effects of each input parameter's variability on the design of flexible pavement.

1.7 Organization of the Thesis:

The thesis is organized into the following five main chapters:

Chapter-1 Introduction: This chapter presents an introduction to the background of the present investigation followed by defining the objectives and scopes available to achieve the same.

Chapter-2 Literature Review: This chapter presents a review of the research literature on the geo-reinforcement of pavement layers and how it affects pavement performance.

Chapter-3 Numerical Analysis and Design Methodology: This chapter deals with the numerical, materials and design methodology of flexible pavement with and without reinforcement that is used for IITPAVE software, such as input parameters and process and output of the method and describes the study area of the project.

Chapter-4 Results and Discussions: This chapter deals with the results and discussion obtained from the numerical analyses.

Chapter-5 Conclusions and Future Scope: This chapter presents a summary of conclusions and the scope of future studies. It presents a summary of the present research and conclusions drawn from the obtained results and also suggests the scope of future study in the related field.

Chapter 2

LITERATURE REVIEW

In recent years, the usage of geosynthetics in the field of civil engineering has increased rapidly. The following sections summarize the selected experimental, analytical and/or numerical studies carried out by various researchers to quantify the effectiveness of geosynthetic reinforcement in pavement construction.

2.1 Experimental study:

The experimental work done by many researchers in the field of geotechnical engineering to increase the stiffness and bearing capacity of the foundation of flexible pavement is discussed in this section. It contains a summary of the research on the effects of geosynthetic reinforcement in flexible pavement subgrade layers.

Al-Qadi et al. (2008) investigated the geogrid effectiveness in a low-volume flexible pavement. Nine pavement test sections are constructed with a base thickness of 203 mm (8in.), 305 mm (12 in.) and 457 mm (18 in.). For these purposes, asphalt thicknesses of 76 mm (3 in.) were used, except in one section, where an asphalt thickness of 127 mm (5 in.) was used. The California Bearing Ratio (CBR) of the subgrade on which the pavement test sections were constructed was four per cent. Based on the results of the accelerated testing, it was determined that inserting geogrid at the subgrade and base course interface improves performance for a thin base course layer and that for a larger base course layer, the geogrid should be placed in the top third of the base course layer. The results reported by (*Henry et al.* 2009) showed a traffic benefit ratio of 1.3 to 1.4. No

benefit was observed in the test section with 600 mm (24 in.) thick base and 150 mm (6 in.) thick asphalt. Variation of longitudinal deflection vs longitudinal distance is shown in Figure 2.1 [14].

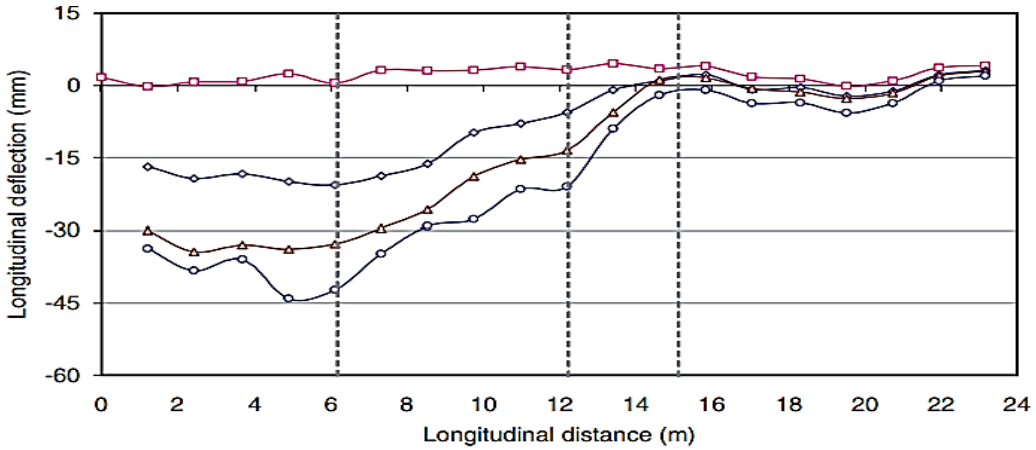

Figure 2.1: Variation of longitudinal deflection vs longitudinal distance [14].

Yang et al. (2014) performed experimental investigations of the behaviour of geogrid-reinforced sand that simulates the reinforcement attached to the wall facings in a variety of in-situ situations and incorporates reinforcement with anchorages. According to experimental findings, both anchored and non-anchored geogrid reinforcements can increase the peak shear strength and reduce the volumetric deformation of reinforced soil when compared to unreinforced specimens. Nearly three times as much of the shear-strength improvement was attributed to geogrid anchorage as to the interaction of the soil with the geogrid in non-anchored specimens [15].

Naeini and Moayed (2009) conducted the California Bearing Ratio tests of three different types of soil samples with different percentages of bentonite with or without geo-grid reinforcement in one or multi-layered**.** The outcome demonstrates that as the soil's plasticity index increases, the California Bearing Ratio values fall in both soaked and un-soaked situations. when compared to

unreinforced soil samples, the California Bearing Ratio is increased by using geo-reinforcement in two layers, however, this CBR value is less than the CBR when the geo-reinforcement is inserted in single-layered reinforcement. When compared to an unreinforced soil sample under both soaked and un-soaked conditions, there was an increase in California Bearing Ratio values with the placement of the geo-reinforcement at the second layer. Placement of two layers of geo-reinforcement at layers 2 and 4, the soaked values of California Bearing Ratio becomes increase by about 35 percent at different plasticity index values when it is compared with an unreinforced soil sample. However, this increase of the CBR value is less when it is compared with geotextiles placed in single layer 3. the soaked CBR value, however, exceeds both the unreinforced and the specimen with one layer of geo-reinforcement. California Bearing Ratio increases by 40% when a single layer of geo-reinforcement is added to the top layer 3 in a saturated condition compared to an unreinforced sample. Thus, placing a single layer of geotextile at layer 3 becomes more effective in soaked conditions [16].

Huang and Menq (1997) conducted an experimental study on geogrid-reinforced lightweight aggregate beds to determine their subgrade modulus. The study's variables included soil density (both compact and very loose), the breadth of the soil reinforcement, the position of the top geogrid layer, the number of geogrid layers, and the tensile strength of the geogrid. The results were compared with the data reported in the literature on geogrid-reinforced sand ceramic beads. It was proposed that it is preferable to have geogrid reinforcement with a width that is four times that of a square or circular footing. The ultimate bearing capacity obtained from the model test program was compared with the theory proposed. For

the same soil, geogrid and its configuration and the ultimate bearing capacity and bearing capacity ratio increased with the increase in embedment ratio $\frac{d_f}{B}$ [17].

Prasad and Kumar (2010) concluded that the geo-reinforcement is added to the gravel subbase that is placed on the expansive subgrade soil, the load-carrying capacity of a model flexible pavement system increases. The depth of the subgrade soil is 500 mm and compacted in ten layers and the gravel subbase is laid in two layers, each of 7 mm compacted thickness. The various reinforced materials, such as waste rubber tyres, bitumen-coated chicken mesh, bitumen-coated bamboo mesh, and geogrid, were uniformly and fully mixed. Two compacted layers of the base material WBM-II, each measuring 75 mm, can be applied. With the application of various forms of reinforcing material, it has been found that the bituminous pavement system's total and elastic deformation values are reduced. When geogrid reinforcement is used, the load-carrying capability is improved. The rebound deflection caused by geogrid is lesser than that caused by any other existing reinforcement material. Pressure vs total deformation is shown in Figure 2.2 [18]and Pressure vs elastic deformation is shown in Figure 2.3 [18].

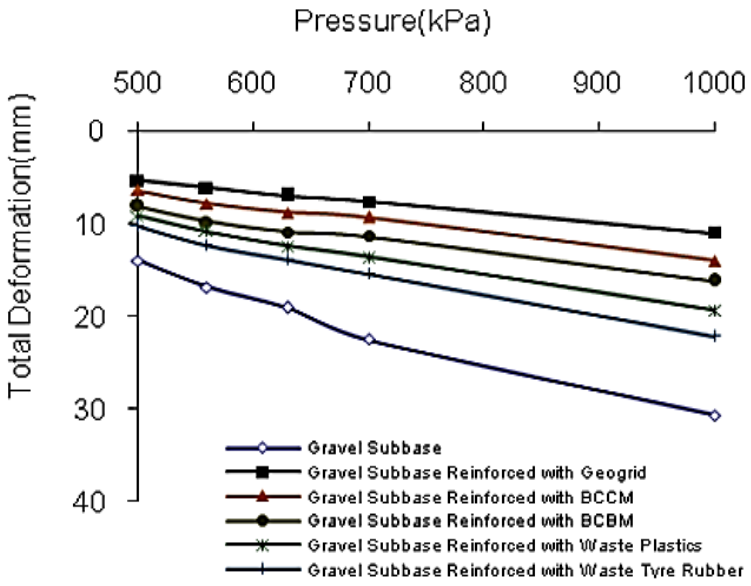

Figure 2.2: Pressure-deformation curves for different pavement stretch laid on expansive soil subgrade [18].

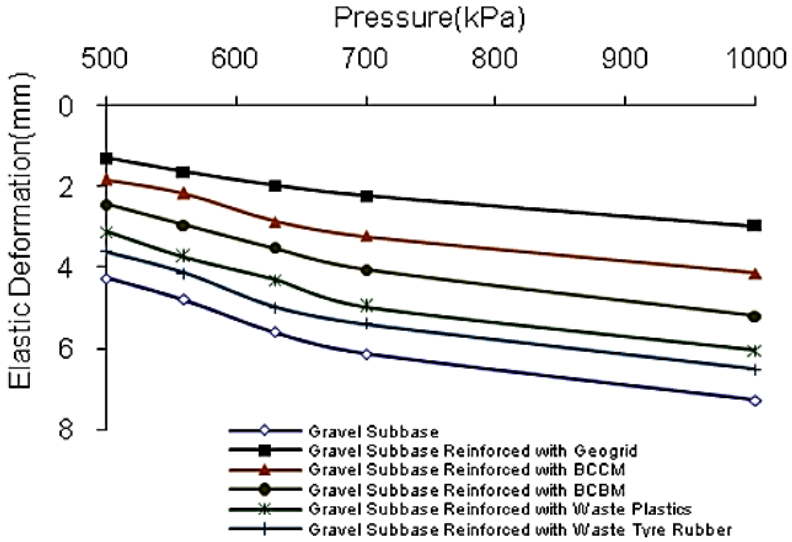

Figure 2.3: Pressure-Elastic deformation curves for Different Pavement Stretches Laid on Expansive Soil Subgrade [18].

Sutharsanam et al. (2010) introduced the Synthetic non-woven geotextile placed at different depths of the soil so that the improvements in soil bearing capacity are checked by CBR and UCS tests. A single layer of geotextile is introduced at the centre (mid-depth) showing that there is an increase of CBR (2.42%) and UCS (0.484N/mm2), better performance than those samples with the geotextiles layer at other depths.[19]

Jha et al. (2011) improved the CBR value of expansive soil subgrade using geosynthetics. The basis of this study is the insertion of multiple layers of reinforcement, including jute and non-woven geotextiles, within the sub-grade soil. It is observed that the placing of a horizontal layer of geotextile within the specimen is effective for controlling the swelling. He found that the expansion ratio of the soil becomes decreases when the geotextile is placed in a single layer of unreinforced soil. This ratio generally drops as the number of reinforcing layers rises, however, these value decreases are significant when jute geotextile is used, while non-woven geotextiles only experience marginal value decreases. It follows

that the placement of geotextile also regulates soil expansion. It has been discovered that as the number of reinforcing layers increases, so does the soil's CBR value. Although jute geotextiles are less durable than non-woven geotextiles, they can nevertheless be beneficial for low-cost road projects [20].

Singh and Gill (2012) carried out the experimental test to determine the optimum position of geogrid/geotextile reinforcement in the subgrade soil by conducting the California Bearing Ratio (CBR) test and unconfined compressive test (UCS). When the geotextile is applied in a single layer, it is discovered that the CBR value of the weak soil increases by 50% to 100%. The position of the geogrid and the value of the unreinforced soil's California Bearing Ratio determine how well the weak subgrade will perform. He discovered that placing geo-grid or geotextile reinforcement at a distance of 0.2H from the top of the mould increases the CBR value to increase from 3.6% for the unreinforced sample to 8.7% for the reinforced sample. Thus, the stress-strain behaviour of subgrade soil under the static load is also improved, when the geotextile is placed at an optimum position. The load vs penetration curve is shown in Figure 2.4 [21].

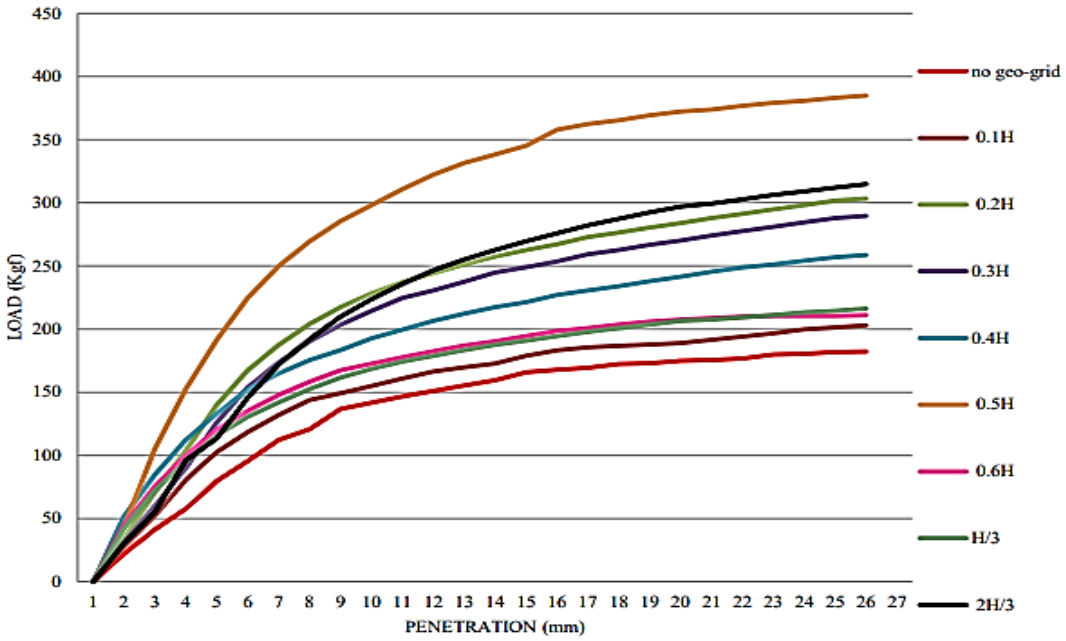

Figure 2.4: load vs. penetration curve for geo-grid reinforced soil with different positions of geo-grid from the top of the specimen [21].

Sarkate et al. (2011), improved the properties of weak subgrade soil and soft murrum with the addition of geogrid in different percentages i.e. 1%, 2%,2.5% and 3%. It has been discovered that the installation of geogrid raises the soil's CBR value as well. She also discovered that murrum 2% of cement with a CBR value of various geogrid percentages. The California Bearing Ratio value of the soil is increased by the addition of 2.5% geogrid. The author used compacted soil samples for performing the laboratory California Bearing Ratio tests. It concluded that the shear strength and permeability of soil are the affecting properties of compaction characteristics [22].

Kumar and Rajkumar (2012) California Bearing Ratio testing is done experimentally in a lab to determine how well woven and non-woven geotextiles function when put between soft subgrade soil and unbound gravel in a bituminous pavement system. A comparison of the reinforcement ratio, as determined by the CBR strength test, is presented. It demonstrates how using woven and non-woven geotextiles improves performance. The author concluded that the reinforcement

ratio is obtained, which is based upon the CBR load penetration relation of both soft subgrade soil-gravel and soft subgrade soil-geotextile-gravel separately, for woven and nonwoven geotextile. Figure 2.5, shows that the reinforcement ratio is more throughout the test, which indicates with the use of geotextiles offers more resistance even to lower penetration, thus the reinforcement ratio increases, with an increase of load in the reinforced soil sample. The reinforcement ratio is taken into account to calculate the improvement in penetration resistance. The variation reinforcement ratio for woven and non-woven geotextile is shown in Figure 2.5 [23].

$$\text{Reinforcement ratio} = \frac{\text{Load with reinforcement}}{\text{load without reinforcement}}$$

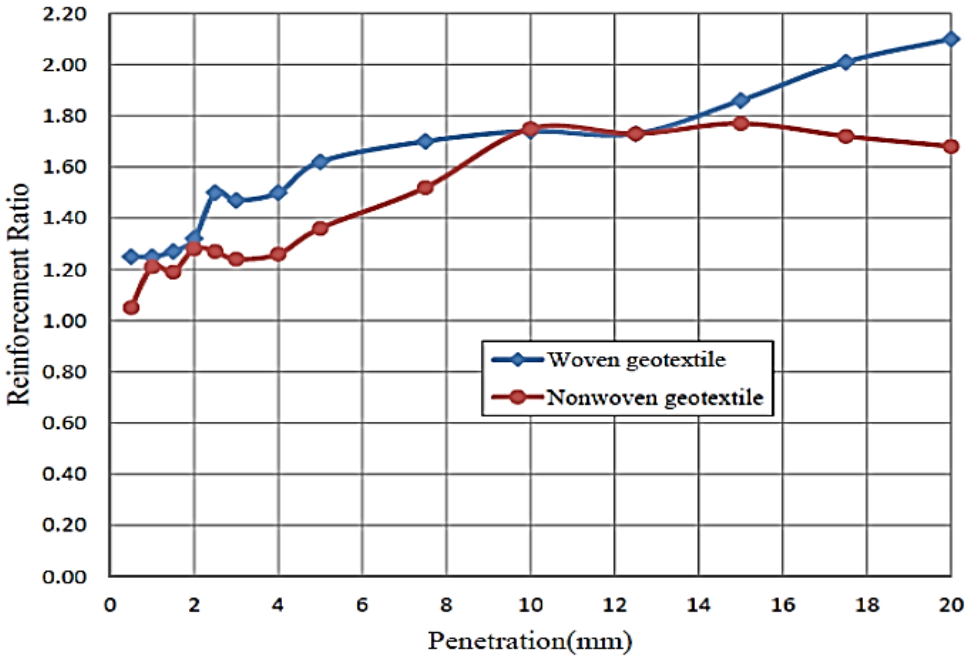

Figure 2.5: Variation of reinforcement ratio for woven geotextile & non-woven geotextile [23].

2.2 Numerical study:

Many researchers have carried out numerical studies to calibrate laboratory and field testing as well as comprehensive analyses of the load transfer mechanism.

Perkins (1999) experimentally verified the reduction in vertical strain in the subgrade and base layer. A base course lateral restraint is the term used to describe the main mechanism responsible for reinforcing paved roadways. The base-courses aggregate moves laterally when vehicular loads are applied to the road surface. Tensile lateral strains are created in the base below the applied load as the material moves down and out away from the load. The geosynthetic restraints the base, thus reducing the lateral movement. The lateral restraint involves several effects of reinforcement including (i) restraint of lateral movement of base aggregate, (ii) increase in base modulus due to confinement, (iii) improved vertical stress on the subgrade due to increased base modulus and (iv) reducing shearing in the top of the subgrade.

Gu Jie (2011) used ABAQUS to model foundation beds and base courses in pavements reinforced with geogrid reinforcement. The soil in the foundation bed was modelled using the Drucker-Prager plasticity model, geogrid was modelled using linear elastic truss elements and soil-geogrid interaction was modelled using two contact surface pairs above and below the reinforcement layer. The bearing capacity of the reinforced foundation bed increased with an increase in the tensile modulus of the reinforcement and the number of layers. Variation of settlement vs pressure is shown in figure 2.6 [24].

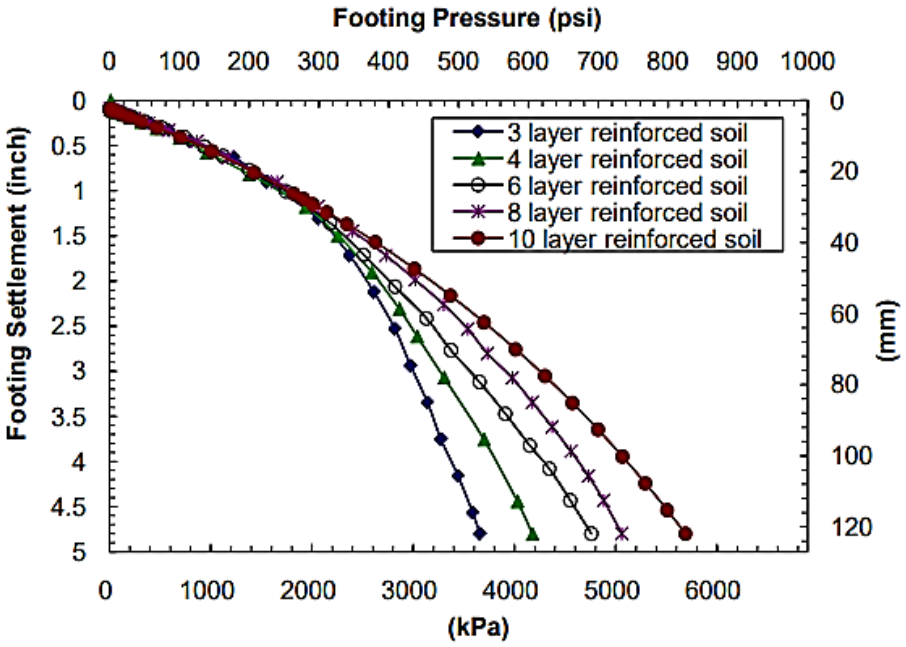

Figure 2.6: Variation of settlement vs pressure [24]

Ennio (2009) developed a finite-element model with the ABAQUS software package to investigate the effect of placing geosynthetic reinforcement within the base course layer on the response of a flexible pavement structure. On various unreinforced and geosynthetic-reinforced flexible pavement sections, finite element computations were carried out. The study's findings showed that the modified critical state two-surface constitutive model could accurately anticipate how the base course material under consideration would react under ideal field conditions when subjected to cyclic and static loads. The results of the finite-element analyses showed that the geosynthetic reinforcement reduced the lateral strains within the base course and subgrade layers. The development of the plastic strains rather than the resilient strains was determined to be where the geosynthetic layer showed the most benefit. As its elastic modulus increased, the benefits of reinforcing became more prominent. Furthermore, Leng and Gabr (2003) used ABAQUS to conduct a numerical analysis to examine the effectiveness of reinforced unpaved pavement sections. The researchers reported that the

performance of the reinforced section was enhanced as the modulus ratio of the aggregate layer to the subgrade decreased. The critical pavement responses were significantly reduced for higher modulus geogrid or better soil/aggregate-geogrid interface properties [25].

Perkins (2001) described a two-dimensional finite element model for the simulation of unpaved road test sections. The reinforcement was modelled as a structural two-node linear elastic membrane element, while the base aggregate was modelled using a nonlinear elastic model. A contact shear interaction model was used for the interface between the reinforcement and base aggregate. They provided damage (rutting) model descriptions for the subgrade and base aggregate layers. The model was calibrated using data from experiments conducted on unpaved road segments using laboratory models [26].

Ahirwar and Mandal. (2017) conducted research to access the functioning of geogrids in the flexible pavement through finite element analysis with PLAXIS 2D software. The finite element analysis results show the reduction in vertical surface deformation when the geogrids were added between the pavement layers. The output results of PLAXIS software show the beneficial effects of the axial stiffness of geogrids in the base course and interface strength of materials at a different thickness of the base course layer on vertical surface deformation. The effect of reinforcement on surface deformation is shown in Figure 2.7 [27].

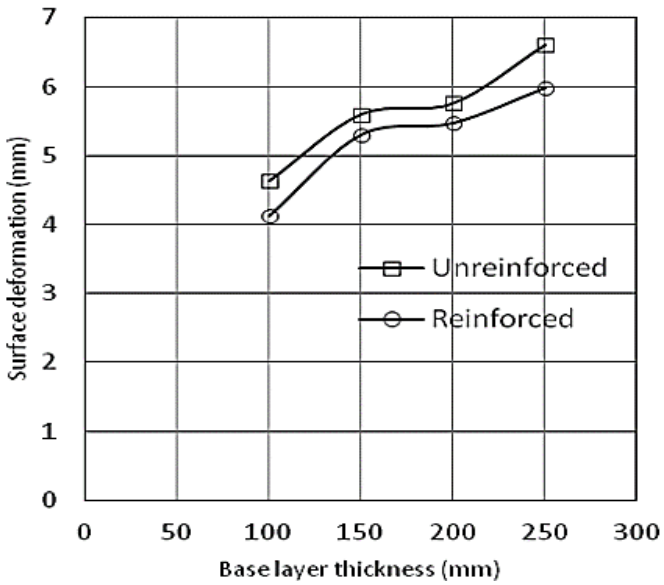

Figure 2.7: Effect of reinforcement on surface deformation [27]

Al-Azzawi (2012) carried out finite element simulations of geogrid through ANSYS software and presented the analysis of soil-geogrid interaction to evaluate the benefits of using geogrid in flexible pavements. According to reports, the bonding between the asphalt concrete and geogrid was improved when it was positioned at the bottom of the base course layer. The effect of the geogrid position on maximum deflection is shown in Figure 2.8 [28].

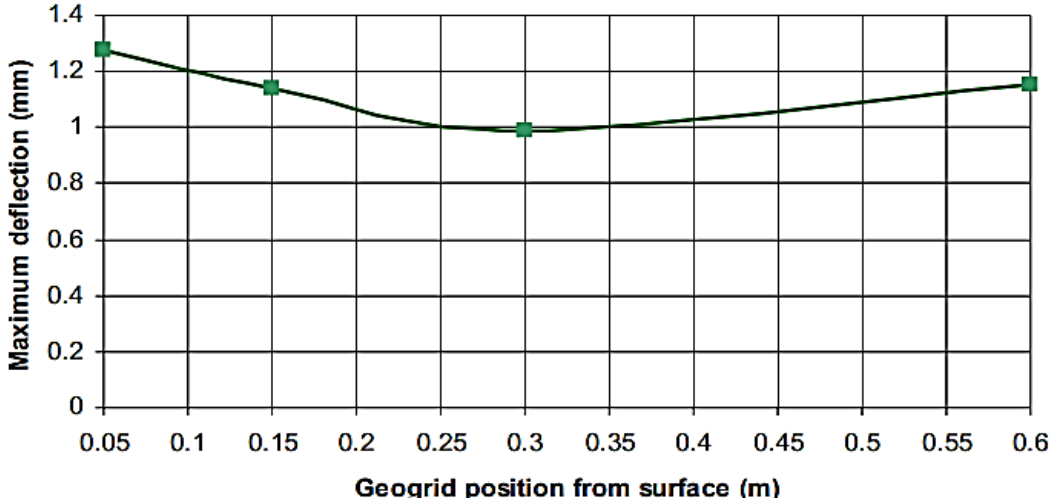

Figure 2.8: Effect of geogrid position on maximum deflection [28]

Chapter 3

NUMERICAL ANALYSIS AND DESIGN

METHODOLOGY

The condition of the materials and the traffic loads have a significant impact on the performance of pavements hence each design contains a different approach. The proposed design approaches for various geosynthetic functions, such as reinforcement, drainage separation, and filtration in the pavement section, are either based on empirical and analytical considerations or analytical models that have been improved by experimental data. There is presently no general analytical design solution that determines all of the various factors that affect performance. All the empirical design methodologies are limited by the conditions connected with the experiments of the study. Many of the approaches produce reliable analysis at a certain set of conditions.

3.1 Design Methods Based on IRC 37:2012

Flexible Pavements are widely used despite some concerns about their economics under various conditions. Soil subgrade and traffic loading are two of the most important factors that affect pavement design. The soil sub-grade strength in terms of California Bearing Ratio and traffic loading in terms of million standard axles (MSA) are the two metrics used by Indian guidelines for the design of flexible pavements.

3.1.1 Empirical design of IRC 37:2012

The proposed methodology takes design traffic into consideration and uses the total number of standard axles as the axle load spectrum for heavy traffic. The load spectrum calculation requires the following parameters:

(i) Initial traffic after construction (in terms of CVPD)

According to IRC 9-1972, a seven-day, 24-hour count should be used to estimate the current average traffic.

(ii) Traffic growth rate during the design period (in percentage)

Forecasting of traffic is done for the next 15 or 20 years, which is the design life of the pavement. The necessary traffic growth rate, as determined by previous studies, however, if information regarding the yearly growth rate of commercial vehicles is unavailable or if it is less than 5%. In the calculation, a growth rate of 5% should be used (as per IRC: SP 84-2009).

$$\text{Traffic prediction, } P_n = P_0\,(1+r)^n \qquad (3.1)$$

Where,

P_n = Traffic (in nth year) P_0 = Traffic flow in the base year

n = Number of years r = Traffic growth (in percentage)

(iii) Design period in a number of years

It is recommended that pavements for state and national highways be designed with a minimum lifespan of 15 years. With the use of creative design and high-fatigue bituminous mixes, expressways and urban roads may be designed for a lifespan of 20 years or more. High-volume roads with design traffic of more than 200 MSA and continuous pavements can also be constructed in light of experience

in India and overseas. A design life of 10 to 15 years may be used for other types of roadways.

(iv) Spectrum of axle loads and vehicle damage factor (VDF)

By carefully performing proper axle load surveys on the existing roadways, VDF is brought into existence. For surveys with a minimum sample size, 10% of commercial vehicles per day or more than 6000. For a divided roadway, the loading pattern may allow for a different pavement thickness in each direction. Since there may be a significant difference in axle loading in two directions of traffic on some sections, VDF is evaluated directionally.

(v) Distribution of commercial traffic over the carriageway

To calculate the total equivalent standard axle load applications to be taken into consideration in the design, the distribution of commercial traffic in each direction and lane must be taken into account. For dual carriageway roads, the design of a dual three-lane carriageway 60% distribution of commercial traffic over the carriageway taken. Finally, the cumulative million standards axles, which are calculated using CVPD, VDF, growth rate, and design life, are provided below.

$$N = \frac{[\![365*\{(1+r)^n-1\}*A*D*F]\!]}{r} \quad (3.2)$$

Where,

N = Cumulative number of standard axles (in terms of MSA)
n = Design life (in years)
r = annual growth rate of commercial vehicles (in decimal)

A = Initial traffic in the year of completion of construction in terms of the commercial vehicle per day (in terms of CPVD)

F = Vehicle damage factor

D = Lane distribution factor (as per IRC 37:2012 para 4.5.1)

3.1.2 Composition of pavement:

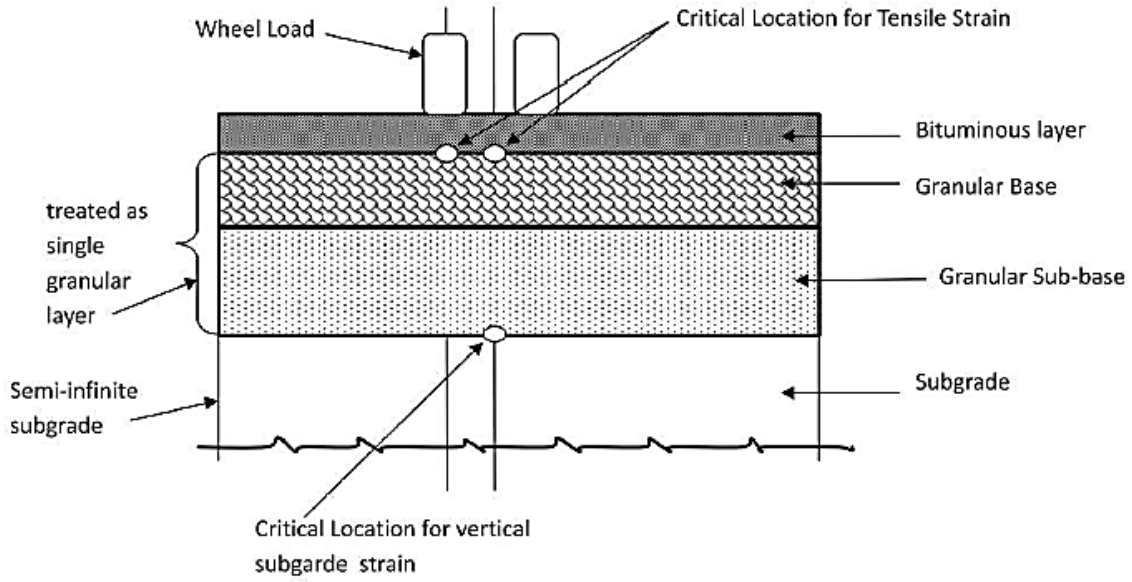

Figure 3.1: Different layers of Bituminous Flexible Pavement [1]

3.2 Upgradation of IRC 37 (2012)

The design process for flexible pavement in early versions of IRC 37 is quite rigid because only a limited number of design catalogues based on empirical formulas were available by the various CBR values and the load spectrum. But, IRC 37:2012 suggests the following design approaches, which are somewhat adaptable and reliable but still require full proofing.

Principles of Pavement Design:

The pavement structure is a multi-layered, linear elastic system, and the E value and μ values characterize the material's stress-strain solution. With the exception of the subgrade layer, each layer has a defined thickness, H1, H2, etc. The pavements should be designed such that they should perform efficiently throughout their design life. When wheel loads are applied to the top surface of the pavement structure, two types of strains may occur, according to pavement analysis.

- Tensile strain, ε_t, at the bottom of the bituminous layer
- Vertical strain, ε_v, on the top of the subgrade layer.

These are the two criteria used in pavement design to prevent rutting and cracking in the bituminous layer. The top surface of the bituminous layer will crack if the critical horizontal tensile strain (ε_t) value exceeds the allowable strain value, and the pavement may distress due to fatigue. If the vertical compressive strain (ε_v) exceeds the allowed strain value, permanent deformation (rutting) will occur on the surface in the pavement structure due to the overloading of the subgrade, and the pavement may distress as a result of the rutting. The three-layered pavement structure and its critical strain are illustrated in Figures 3.2 [13]and 3.3 [1].

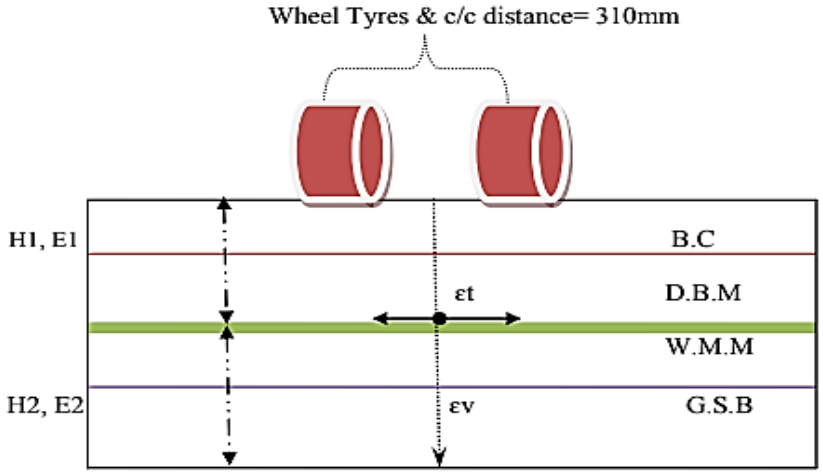

Figure 3.2 pavement structure [13]

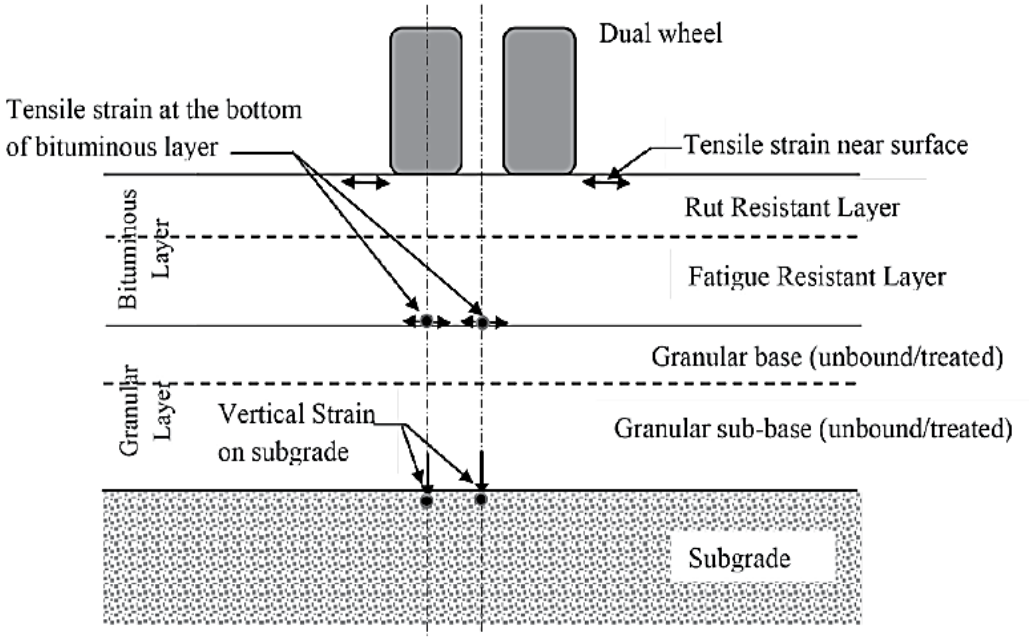

Figure 3.3 Pavement sections with bituminous, GB and GSB showing the locations of critical strains [1]

- ***Fatigue Model:***

According to the IRC: 37-2012, the two equations for the fatigue model at 80% and 90% reliability are given below:

$$N_f = 2.21*10^{-04} * [\frac{1}{\varepsilon_t}]^{3.89} * [\frac{1}{M_R}]^{0.854} \quad \text{[for 80\% reliability]} \quad (3.3)$$

$$N_f = 2.021*10^{-04} * [\frac{1}{\varepsilon_t}]^{3.89} * [\frac{1}{M_R}]^{0.854} \quad \text{[for 90\% reliability]} \quad (3.4)$$

Where,

N_f= Fatigue life in MSA

ε_t= Maximum Tensile strain at the bottom of the bituminous layer

M_R = Resilient Modulus of the bituminous layer

Equation 3.3 gives, fatigue life for 20 per cent cracked area of the bituminous layer at a reliability level of 80% respectively at the end of the design period. In equation

3.4, only ten per cent of the area may have 20 per cent cracks, if 90% reliability is used for high-volume highways. To avoid frequent maintenance, a reliability level of 90 per cent is recommended for highways having design traffic exceeding 30 MSA.

- ***Rutting Model:***

According to the IRC: 37-2012, the two equations for the rutting model at 80% and 90% reliability are given below:

$$N_R = 4.1656*10^{-08} * [\frac{1}{\varepsilon_z}]^{4.5337} \quad \text{[for 80\% reliability]} \qquad (3.5)$$

$$N_R = 1.41*10^{-08} * [\frac{1}{\varepsilon_z}]^{4.5337} \quad \text{[for 90\% reliability]} \qquad (3.6)$$

Where,

N_R = Rutting life in MSA
ε_z = Vertical compressive strain

The limiting rutting is recommended as 20 mm in 20% of the length for design traffic up to 30 MSA and 10% of the length for the design traffic beyond these guidelines offer a design catalogue giving pavement compositions for a variety of traffic conditions, layer configurations, and assumed material qualities. The design can be immediately adopted from the relevant design charts provided in the catalogue if the designer decides to employ any of these combinations and is satisfied that the layer properties assumed in the design catalogue can be achieved in the field.

3.3 Design of Geogrid Reinforced Flexible Pavements:

The design of geogrid-reinforced pavement is strongly based on the condition of different soil layers, geogrid properties, and traffic loads, and therefore, each

design needs special analysis and calculations. A standard design approach (Mechanistic-Empirical Pavement Design Guide) for the analysis and design of conventional pavement has gained widespread acceptance due to its numerous advantages over the empirical approach. This mechanistic-empirical technique was used in IRC 37 for the analysis and design of flexible pavement. Indian roads congress (IRC 37) has specified the design catalogues for flexible pavements based on different traffic loads (in terms of million standard axles, MSA) and CBR values of the subgrade. According to the design approach given in IRC 37, the Tensile strain, ε_t, at the bottom of the bituminous layer and the vertical subgrade strain, ε_v, on the top of the subgrade is considered to be the critical parameters for pavement design to restrict cracking and rutting in the bituminous and non-bituminous layer respectively.

The detailed design philosophy for the design of geogrid-reinforced flexible pavement is illustrated as follows:

Step 1: For the design of geogrid-reinforced flexible pavement, the thickness of various pavement layers such as subgrade, sub-base, base, and bitumen layer is taken from the design catalogue given in IRC:37 corresponding to CBR value and traffic load.

Step 2: Calculation of resilient modulus of subgrade and different layers of pavement is done based on the empirical relation as given in IRC:37, as illustrated below.

$M_{Bitumrn} = 2000\ MPa$, for traffic load up to 20 MSA

$M_{Bitumrn} = 3000\ MPa$, for traffic load exceeding up to 20 MSA

$$M_{Granular} = 0.2 \times h^{0.45} \times M_{Support} \quad (3.7)$$

$$M_{Support} = \frac{2(1-\mu^2)pa}{\delta} \quad (3.8)$$

$$M_{RS} = 10.0 \times CBR, \quad \text{for CBR} \leq 5\% \quad (3.9)$$

$$M_{RS} = 10.0 \times CBR^{0.64} \quad \text{for CBR} \geq 5\% \quad (3.10)$$

Step 3: For unreinforced pavement, stresses, strains, and deflections at the selected critical locations are obtained from numerical analyses using the input value of the modulus of different layers of pavement, their thicknesses, and Poisson's ratio as recommended by IRC 37. If the obtained strain values are within the limiting strain values, then the pavement composition is considered to be safe.

Step 4: Now, the limiting strain values are calculated from the rutting and fatigue model which are given in IRC 37. The rutting and fatigue models as given in IRC are discussed above.

Step 5: Now, to design a geogrid-reinforced pavement, the geogrid is introduced at the base layer of the pavement and numerical analyses have been carried out. The vertical compressive strain on the subgrade is calculated for the reinforced case and the obtained strain will be less than the unreinforced section.

Step 6: Based on the vertical compressive strain on subgrade in the case of the reinforced and unreinforced pavement, the service life ratio is obtained, SLR = $\frac{\varepsilon_{v1}}{\varepsilon_{v2}}$

Step 7: By repeated trials and back calculations method, in the case of reinforced pavement, the height of the base layer is reduced based on the equal subgrade strain value of the unreinforced pavement model. Using the value of reduced base layer thickness, the resilient modulus of the base layer for reinforced pavement is determined as per the formulae discussed above.

Step 8: Furthermore, using the same base layer thickness for both the unreinforced and reinforced pavement sections as given in IRC:37 for different values of CBR and traffic loads, the surface deflection was obtained through numerical analyses. Then, the effective resilient modulus of the supporting layer is computed using the obtained deflection values as explained above. Then, the resilient modulus of both reinforced and unreinforced base layers is again calculated with the value of the supporting layer.

3.3.1 Strength Characteristics

A soil that has been reinforced with a material that can withstand tensile loads and interact with the soil through friction and/or adhesion is referred to as reinforced soil. The result of the reinforcement can be seen as a restraint, resisting expansion caused by generated normal or shear stresses. It is possible to imagine that the reinforcement acts as a normal stress $\boldsymbol{\sigma_R}$ the direction of the reinforcement, preventing the soil mass from expanding. Alternately, the reinforcement may be thought of as exposing the soil to shear stresses τ_R. These two methods for modelling the increase of strength according to Hausmann (1976), the SIGMA- and TAU-models for reinforced soil were used [29].

$$\boldsymbol{C_R = \frac{\sigma_R}{2\sqrt{K_a}}}$$

3.4 Numerical Modeling

This section briefly discusses the numerical analysis of unreinforced and reinforced (i.e., geogrid) flexible pavements using IITPAVE software. For

evaluation of the results based on numerical analysis, a mechanistic-empirical software program IITPAVE is used as the benchmark for the problems.

3.4.1 Salient Features of IITPAVE

IITPAVE software has been developed for the analysis of linear elastic layered pavement systems. The stresses, strains and deflections caused at different locations in pavement by a uniformly distributed single load applied over a circular contact area at the surface of the pavement can be computed using this software. The effect of additional loads (which should also be uniformly distributed loads over circular contact areas) was considered using the superposition principle. The single vertical load applied at the surface is described in terms of (a) contact pressure and radius of contact area or (b) Wheel load and contact pressure or (c) Wheel load and radius of the contact area. For IITPAVE, wheel load and contact pressure are the load inputs. The pavement inputs required are the elastic properties (elastic/resilient moduli and Poisson's ratio values of all the pavement layers) and the thicknesses of all the layers (excluding subgrade). IITPAVE software, in its current version, can be used to analyse pavements with a maximum of ten layers including the subgrade. If the number of layers in the pavement is more than ten, different layers of similar nature (eg. granular, bituminous) can be combined and considered as one layer. A cylindrical coordinate system is followed in the program. Thus, the location of any element in the pavement is defined by (a) the depth of the location of the element from the surface of the pavement and (b) the radial distance of the element measured from the vertical axis of symmetry (along the centre of the circular contact).

3.4.2 IITPAVE - For Analysis of Flexible Pavement

IITPAVE software, developed by IIT Kharagpur, is an elastic multilayer linear analysis tool that is used to find out stress, strains, and deflection for a standard axle load were computed using this software at the critical points

The following steps may be followed for analysing flexible pavements using IITPAVE

(i) Open IRC_37_IITPAVE folder.

(ii) Double-click on IITPAVE_EX.exe file in the IRC_37_IITPAVE folder. IITPAVE start screen will appear as shown in Figure 3.3 [1].

(iii) From the Home screen user can manually give input through the input window by clicking on 'Design New Pavement Section'. Users can also give input through properly formatted input files by clicking on the 'Edit Existing File' option and then browsing and opening the input file, shown in Figure 3.4 [1].

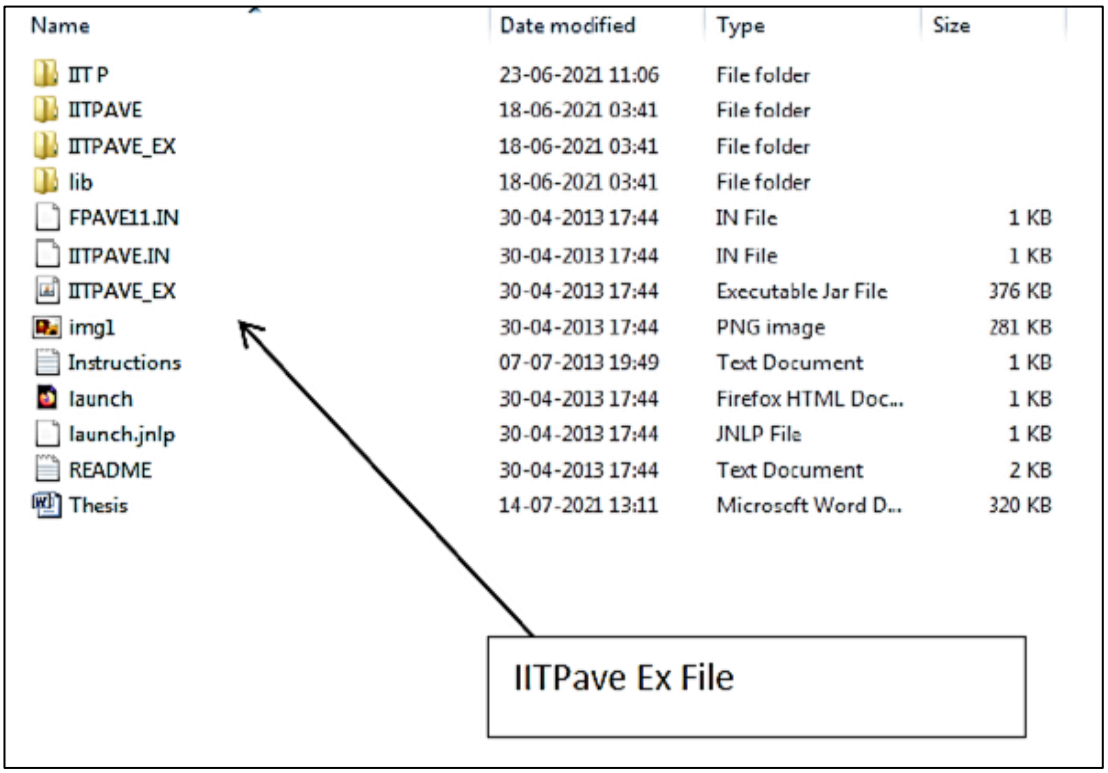

Figure 3.3 IITPAVE Ex File [1]

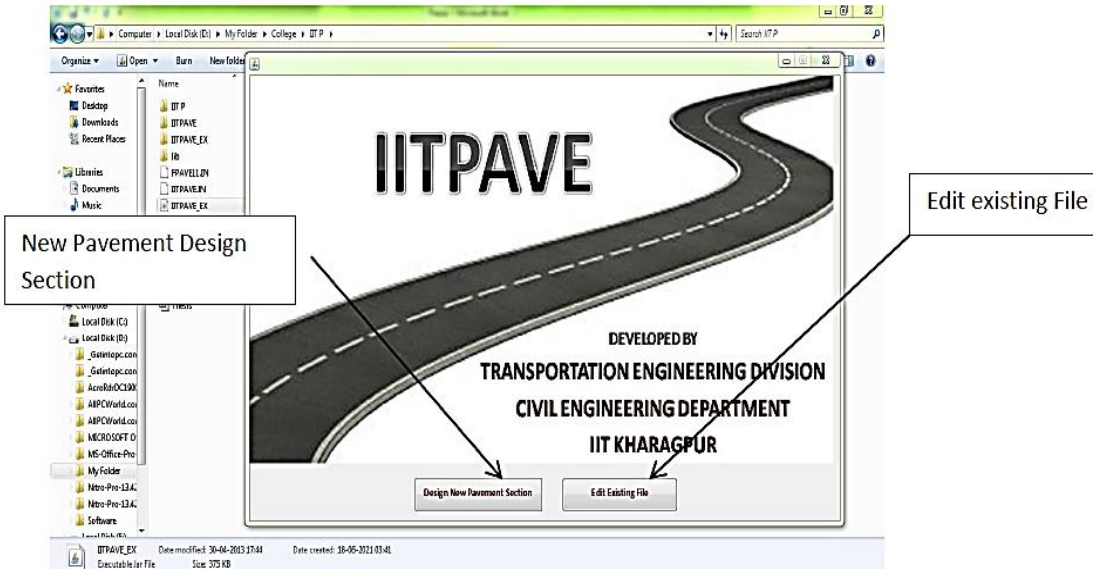

Figure 3.4 New pavement design section and edit existing file [1]

(iv) Next, an input window will come. All the inputs required have to be given through that input window, shown in Figure 3.5 [1].

(v) First, a number of layers are to be selected from the drop-down menu to fix up input boxes for different layers.

(vi) Next, Elastic modulus (E) values of the various layers in MPa, Poisson's ratio and thickness of the layers in mm excluding the sub-grade thickness are to be provided.

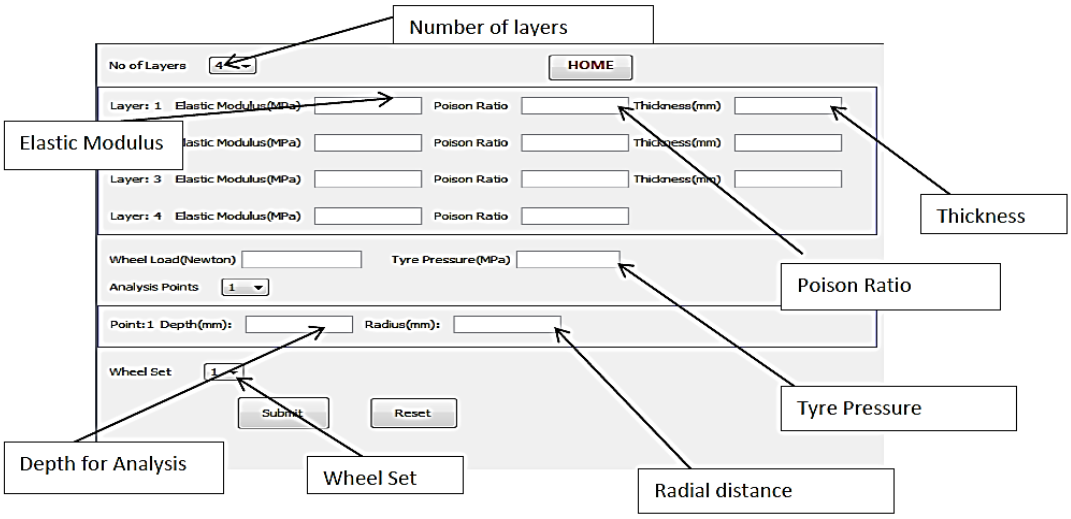

Figure 3.5: Input window [1].

Single wheel load and the tyre pressure are to be provided (tyre pressure of 0.56 MPa has been used for calibration of the fatigue equation and the same pressure. can be used for stress analysis. Change of pressure even up to 0.80 MPa has a small effect on stress values in lower layers.)

(vii) Then the number of points for stress computations is to be given through the dropdown menu for Analysis points.

(viii) Then corresponding to different points, the values of depth Z in mm and the corresponding value of radial distances from centre (r) in mm are to be given (wheel centre to centre distance of 310 mm is considered).

(ix) Provide whether an analysis is for single-wheel load or double-wheel load by clicking 1 or 2. This will be the most common case.

(x) The output of the program will provide stresses, strains and deflections at the desired points. Next check if the computed strains are less than the permissible strain in the VIEW HERE icon. If not, then click BACK TO EDIT and run the program with a new thickness combination till the permissible strain values are achieved. epT, epR and epZ will be the outputs that will be of interest. For the cemented base, tensile stress at the bottom of the cemented layer SigmaT / SigmaR is needed for cumulative fatigue damage analysis.

(xi) In most cases the tensile strain at the bottom of the bituminous layer is higher in the longitudinal direction (epT) rather than in the radial direction (epR). If tensile strain in the bituminous layer is high, increase the thickness of the bituminous layer.

(xii) Tensile strains in the cementitious bases also are to be computed for design. If the Tensile strain/stress in the cemented layer is higher, increase the thickness of the Cemented layer.

(xiii) Vertical sub-grade strain (epZ) should be less than the permissible value for the design traffic. If the vertical sub-grade strain is higher, increase the thickness of the sub-base layer (Figure 3.6).

(xiv) Stress values can also be easily computed by changing directly the input file which is to be written in an illustrated in the manual and browsing the input file by clicking 'Edit Existing File on the home screen of IITPAVE'.

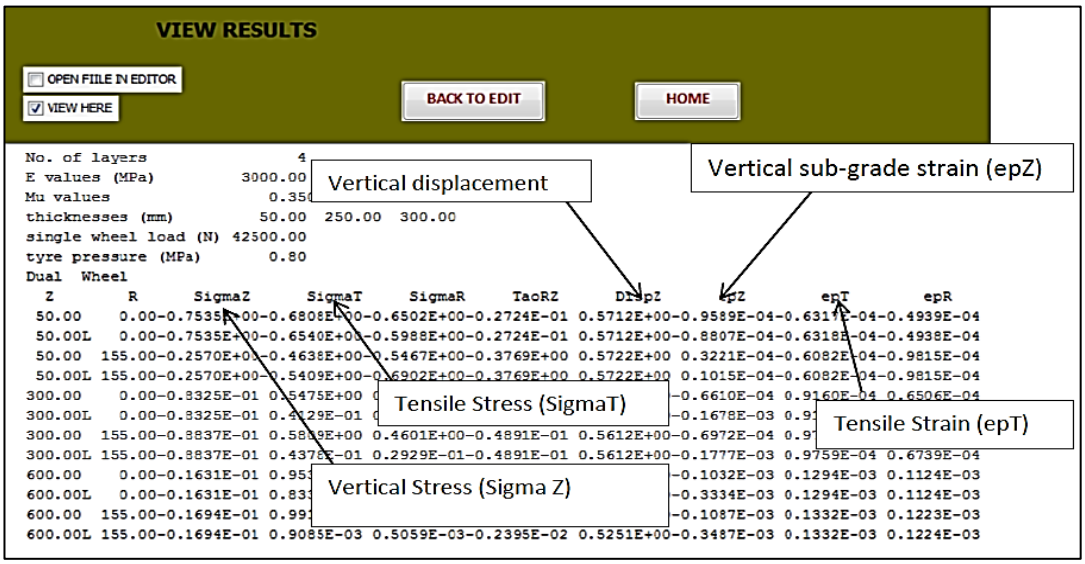

Figure3.6: Output Results of IITPAVE [1]

3.4.3 Material properties

As discussed in the previous chapter, input parameters and their variability play a major role in designing flexible pavement.

Layer Modulus

The resilient modulus of all the materials (Bituminous/Asphalt concrete, granular base and sub-grade) was considered to be log-normally distributed. This conclusion was drawn based only on the data literature review. Since those specified parameters would determine the input variability for a particular design,

this report was simply meant to quantify the range of practical variability for each of the materials.

According to IRC 37:2012 (Shown in Table 3.1, the bituminous layer's resilient modulus varies significantly with temperature. As temperature changes have the greatest impact on the top layer of the pavement, for this project, only the bituminous layer's resilient modulus is considered.

Table 3.1 Resilient modulus of bituminous mixes

Mix type	**Average Annual Pavement Temperature** ℃				
	20	25	30	35	40
BC and DBM for VG10 bitumen	2300	2000	1450	1000	800
BC and DBM for VG30 bitumen	3500	3000	2500	2000	1250
BC and DBM for VG40 bitumen	6000	5000	4000	3000	2000
BC with modified bitumen	5700	3800	2400	1600	1300
BC with VG10 bitumen	500 MPa at 35 ℃				
BC with VG10 bitumen	700 MPa at 35 ℃				
RAP treated with 4 per cent bitumen emulsion/ foamed bitumen with 2-2.5 per cent residual bitumen and 1.0 per cent cementitious material.	800 MPa at 35 ℃				

Poisson’s Ratio:

The literature analysis revealed that the impact of numerous factors on Poisson's ratio is typically minor. In order to be consistent with what was found in the literature review, it was decided to fix Poisson's ratios (Table 3.2) for the three primary types of materials.

Table 3.2 Typical values of Poisson’s ratio

Layer	Poisson's ratio
Bituminous	0.35
Granular	0.35
Subgrade	0.35

Layer thickness:

According to the literature review, it is not possible to construct pavement layers exactly the same thickness as the design thickness. According to certain studies in the literature, thickness is normally distributed.

Table:3.3 Traffic data

CBR (%)	Traffic (MSA)	Single wheel Load (N)	Tyre Pressure (MPa)
5	100	20000	0.56

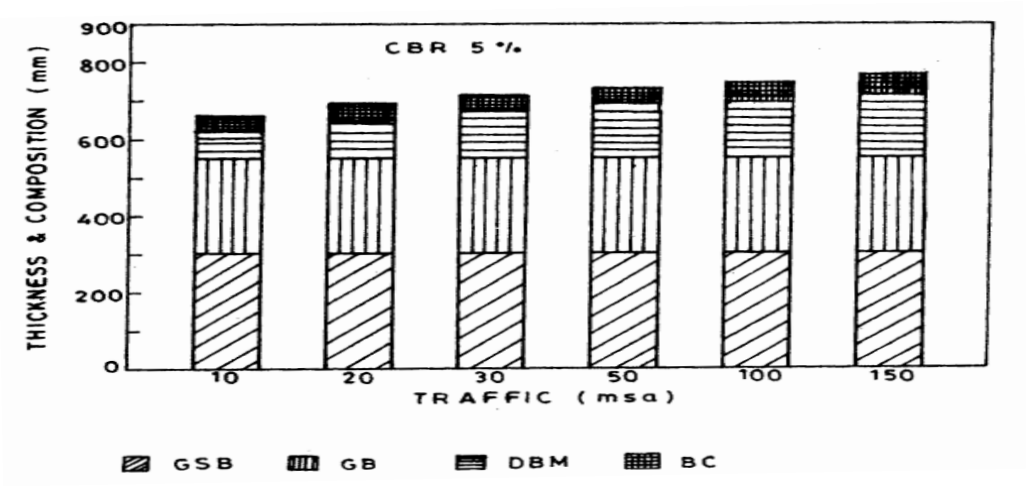

Fig.3.7: Plate-2 (IRC:37-2012) Pavement Design Catalogues

Table:3.4 Properties of soil

Layer	Unit weight (KN/m^3)	φ (°)	c (kPa)
Granular	22	50	0.01
Subgrade	18	26	46

Table:3.5 Properties of geogrid

Model	Sigma-Tau
Material	Elastic
Stiffness (KN/m)	20

This chapter discusses the materials properties and design methodology. The effect of various parameters studied includes granular subbase depth, material behaviour of geogrid. The influence of these parameters on the bearing capacity and stiffness on geogrid is illustrated in Table 3.5.

Chapter 4

RESULTS AND DISCUSSION

4.1 General:

In this chapter, the pavement test sections were designed according to the IRC37-2012 [2] guidelines based on the material properties (CBR=5%) and traffic 100 MSA. In the preceding chapters, chapter 3 describes the details of the Mechanistic-Empirical method of flexible pavement with geosynthetics reinforced and without reinforced. To evaluate the improvement achieved by the geogrid reinforcement, two cases were analysed, namely, the unreinforced flexible pavement and the geogrid-reinforced pavement.

4.2 Results:

In this simulation, structural analysis of flexible pavement is carried out using this IITPAVE software, with required inputs such as the layer thicknesses, moduli, Poisson's ratio values, the standard axle load of 80 KN distributed on four wheels

(20 KN on each wheel), and tyre pressure as 0.56 MPa. Since the analysis is performed for the standard axle of 80 KN, an effective single-wheel load of 40,000 N is given as an input parameter. The estimation of resilient subgrade modules for different pavement layers is done based on the empirical relationship, as illustrated in Table 3.1

The tensile strain and vertical subgrade strain are evaluated for CBR of 5% and traffic load of 100 MSA. The obtained value of tensile strain and vertical subgrade strain is shown in Table 4 and Table 4. For 90% reliability, the limiting value of tensile strain is $170*10^{-06}$ and the vertical subgrade strain is $319*10^{-06}$.

Table 4: Pavement Composition of soil with geo-reinforcement (geogrid) for Rutting life 100 MSA at 90% reliability:

Sl.no	CBR	Granular layer thickness (mm)	DBM (mm)	BC (mm)	Total thickness (mm)	Actual ε_z*	Actual ε_t*1	Allowable ε_z**	Allowable ε_t**2	Rutting life (MSA)	% saving in granular layer thickness	% saving in overall layer thickness
1	5	550	150	50	750	191.0	141	319	170	100	0	0
2	5	550	150	50	750	26.11	143	319	170	100	0	0
3	5	350	150	50	550	57.70	1162	319	170	100	36.36	26.66
4	5	150	150	50	350	141.0	168	319	170	100	72.72	80.00
5	5	100	150	50	300	187.0	169.2	319	170	100	81.81	86.66

*Vertical Strain in microns (10^{-06})

**Allowable Vertical Strain Values in microns (10^{-06})

Table 4.1: The output result from IITPAVE in Native Case for rutting of CBR=5%

No. of layers		3							
E values (MPa)		3000.00	350.00	49.30					
Mu values		0.35	0.35	0.35					
thicknesses (mm)		200.00	550.00						
single wheel load (N)		20000.00							
tyre pressure (MPa)		0.56							
Dual Wheel									
Z	R	SigmaZ	SigmaT	SigmaR	TaoRZ	DispZ	epZ	epT	epR
750	0	-8.55E-03	3.37E-02	3.13E-02	-1.07E-03	2.53E-01	-8.94E-05	7.36E-05	6.44E-05
750.00L	0	-8.53E-03	7.48E-04	5.11E-04	-1.07E-03	2.53E-01	-1.82E-04	7.22E-05	6.57E-05
750	155	-8.53E-03	3.51E-02	3.36E-02	-1.27E-03	2.56E-01	-9.41E-05	7.54E-05	7.01E-05
750.00L	155	-8.53E-03	8.21E-04	6.27E-04	-1.27E-03	2.56E-01	-1.91E-04	7.53E-05	7.01E-05

Vertical strain in micron = 191 x 10^{-06}

Table 4.2: The output result from IITPAVE in Case 1 for rutting of CBR=5%

No. of layers		3							
E values (MPa)		3000.00	16484.86	49.30					
Mu values		0.35	0.35	0.35					
thicknesses (mm)		200.00	550.00						
single wheel load (N)		20000.00							
tyre pressure (MPa)		0.56							
Dual Wheel									
Z	R	SigmaZ	SigmaT	SigmaR	TaoRZ	DispZ	epZ	epT	epR
750	0	-1.46E-03	-1.58E-01	1.53E-01	-8.54E-05	1.10E-01	-6.70E-06	6.40E-06	5.95E-06
750.00L	0	-1.46E-03	-3.10E-04	-3.27E-04	-8.56E-05	1.10E-01	-2.51E-05	6.40E-06	5.95E-06
750	155	-1.52E-03	1.65E-01	1.65E-01	-1.03E-04	1.09E-01	-7.11E-06	6.54E-06	6.55E-06
750.00L	155	-1.52E-03	-3.19E-04	-3.19E-04	-1.03E-04	1.09E-01	-2.62E-05	6.54E-06	6.55E-06

Vertical strain in micron = 26.11 x 10^{-06}

Table 4.3: The output result from IITPAVE in Case 2 for rutting of CBR=5%

No. of layers		3							
E values (MPa)		3000.00	16484.86	49.30					
Mu values		0.35	0.35	0.35					
thicknesses (mm)		200.00	350.00						
single wheel load (N)		20000.00							
tyre pressure (MPa)		0.56							
Dual Wheel									
Z	R	SigmaZ	SigmaT	SigmaR	TaoRZ	DispZ	epZ	epT	epR
550	0	-3.11E-03	3.05E-01	2.88E-01	-2.04E-04	1.59E-01	-1.28E-05	1.24E-05	1.11E-05
550.00L	0	-3.00E-03	-7.01E-04	-7.49E-04	-2.04E-04	1.59E-01	-5.06E-05	1.24E-05	1.11E-05
550	155	-3.11E-03	3.22E-01	3.05E-01	-2.32E-04	1.61E-01	-1.35E-05	1.31E-05	1.17E-05
550.00L	155	-3.11E-03	-7.07E-04	-7.58E-04	-2.71E-04	1.61E-01	-5.27E-05	1.31E-05	1.17E-05

Vertical strain in micron = 52.70 x 10^{-06}

Table 4.4: The output result from IITPAVE in Case 3 rutting of CBR=5%

No. of layers		3							
E values (MPa)		3000.00	16484.86	49.30					
Mu values		0.35	0.35	0.35					
thicknesses (mm)		200.00	150.00						
single wheel load (N)		20000.00							
tyre pressure (MPa)		0.56							
Dual Wheel									
Z	R	SigmaZ	SigmaT	SigmaR	TaoRZ	DispZ	epZ	epT	epR
350	0	-8.32E-03	7.85E-01	6.56E-01	-6.65E-04	2.70E-01	-3.03E-03	3.17E-05	2.41E-05
350.00L	0	-8.83E-03	2.23E-03	-2.50E-03	-6.65E-04	2.70E-01	-1.35E-02	3.17E-05	2.41E-05
350	155	-8.62E-03	7.92E-01	7.01E-01	-1.08E-03	2.73E-01	-3.22E-05	3.33E-05	2.59E-05
350.00L	155	-8.62E-03	-2.26E-03	-2.53E-03	-1.08E-03	2.73E-01	-1.41E-04	3.33E-05	2.59E-05

Vertical strain in micron = 141.0 x 10^{-06}

Table 4.5: The output result from IITPAVE in Case 4 for rutting of CBR=5%

No. of layers		3							
E values (MPa)		3000.00	16484.86	49.30					
Mu values		0.35	0.35	0.35					
thicknesses (mm)		200.00	100.00						
single wheel load (N)		20000.00							
tyre pressure (MPa)		0.56							
Dual Wheel									
Z	R	SigmaZ	SigmaT	SigmaR	TaoRZ	DispZ	epZ	epT	epR
300	0	-1.15E-02	9.88E-01	8.51E-01	-9.50E-04	3.18E-01	-3.97E-05	4.21E-05	3.09E-05
300.00L	0	-1.15E-02	-3.24E-03	-3.66E-03	-9.50E-04	3.18E-01	-1.85E-04	4.21E-05	3.09E-05
300	155	-1.20E-02	1.04E+00	8.83E-01	-1.72E-03	3.22E-01	-4.15E-05	4.44E-05	3.18E-05
300.00L	155	-1.20E-02	-3.35E-03	-3.81E-03	-1.72E-03	3.22E-01	-1.93E-04	4.44E-05	3.18E-05

Vertical strain in micron = 193.0 x 10^{-06}

Table 5: Pavement Composition of soil with geo-reinforcement (geogrid) for Rutting life and Fatigue life 100 MSA at 80% reliability:

Table 5.1: The output result from IITPAVE in the Native case for rutting of CBR=5%

No. of layers		3							
E values (MPa)		1700.00	350.00	49.30					
Mu values		0.35	0.35	0.35					
thicknesses (mm)		200.00	550.00						
single wheel load (N)		20000.00							
tyre pressure (MPa)		0.56							
Dual Wheel									
Z	R	SigmaZ	SigmaT	SigmaR	TaoRZ	DispZ	epZ	epT	epR
200	0	-1.12E-01	2.51E-01	1.87E-01	-1.74E-02	3.45E-01	-1.56E-04	1.32E-04	8.15E-05
200.00L	0	-1.12E-01	3.80E-03	-9.28E-03	-1.74E-02	3.45E-01	-3.14E-04	1.32E-04	8.15E-05
200	155	-1.03E-01	2.31E-01	1.03E-01	-5.63E-02	3.52E-01	-1.29E-04	1.36E-04	3.45E-05
200.00L	155	-1.03E-01	3.79E-03	-2.25E-02	-5.63E-02	3.52E-01	-2.74E-04	1.36E-04	3.45E-05
750	0	-9.53E-03	3.71E-02	3.47E-02	-1.26E-03	2.68E-01	-9.91E-05	8.08E-05	7.16E-05
750.00L	0	-9.53E-03	8.50E-04	4.58E-04	-1.26E-03	2.68E-01	-2.02E-04	8.16E-05	7.09E-05
750	155	-9.96E-03	3.91E-02	3.73E-02	-1.51E-03	2.72E-01	-1.04E-04	8.42E-05	7.76E-05
750.00L	155	-9.96E-03	8.94E-04	6.52E-04	-1.51E-03	2.72E-01	-2.13E-04	8.42E-05	7.76E-05

Vertical strain in micron = 213 x 10^{-06}

Table 5.2: The output result from IITPAVE in Case 1 for rutting of CBR=5%

No. of layers		3							
E values (MPa)		1700.00	16484.86	49.30					
Mu values		0.35	0.35	0.35					
thicknesses (mm)		200.00	550.00						
single wheel load (N)		20000.00							
tyre pressure (MPa)		0.56							
Dual Wheel									
Z	R	SigmaZ	SigmaT	SigmaR	TaoRZ	DispZ	epZ	epT	epR
200	0	-2.41E-01	-1.31E-01	-1.33E-01	-1.63E-02	1.17E-01	-8.71E-05	-1.39E-07	-1.68E-06
200.00L	0	-2.41E-01	-1.43E-01	-1.62E-01	-1.63E-02	1.17E-01	-8.10E-06	-1.40E-07	-1.68E-06
200	155	-1.77E-01	-1.00E-01	-1.07E-01	-1.13E-01	1.16E-01	-6.17E-05	-4.23E-07	-5.76E-06
200.00L	155	-1.77E-01	-1.41E-01	-2.06E-01	-1.13E-01	1.16E-01	-3.37E-06	-4.23E-07	-5.76E-06
750	0	-1.56E-03	1.66E-01	1.61E-01	-9.08E-05	1.14E-01	-7.06E-06	6.72E-06	-6.28E-06
750.00L	0	-1.56E-03	-3.36E-04	-3.53E-04	-9.08E-05	1.14E-01	-2.66E-05	6.73E-06	6.28E-06
750	155	-1.62E-03	1.74E-01	1.74E-01	-1.04E-04	1.13E-01	-7.48E-06	6.89E-06	6.87E-06
750.00L	155	-1.62E-03	-3.48E-04	-3.48E-04	-1.07E-04	1.13E-01	-2.78E-05	6.89E-06	6.87E-06

Vertical strain in micron = 27.8 x 10^{-06}

Table 5.3: The output result from IITPAVE in Case 2 for rutting of CBR=5%

No. of layers		3							
E values (MPa)		1700.00	16484.86	49.30					
Mu values		0.35	0.35	0.35					
thicknesses (mm)		200.00	350.00						
single wheel load (N)		20000.00							
tyre pressure (MPa)		0.56							
Dual Wheel									
Z	R	SigmaZ	SigmaT	SigmaR	TaoRZ	DispZ	epZ	epT	epR
200	0	-2.36E-01	-1.40E-01	-1.41E-01	-1.87E-02	1.70E-01	-8.12E-05	-4.61E-06	-5.70E-06
200.00L	0	-2.36E-01	-2.51E-01	-2.65E-01	-1.87E-02	1.70E-01	-3.39E-06	-4.61E-06	-5.70E-06
200	155	-1.73E-01	-1.10E-01	-1.15E-01	-1.16E-01	1.73E-01	-5.55E-05	-5.24E-06	-9.73E-06
200.00L	155	-1.73E-01	-2.55E-01	-3.10E-01	-1.16E-01	1.73E-01	1.51E-06	-5.24E-06	-9.73E-06
550	0	-3.31E-03	3.30E-01	3.12E+01	-2.22E-04	1.68E-01	-1.38E-05	1.34E-05	1.19E-05
550.00L	0	-3.32E-03	-7.96E-04	-8.15E-04	-2.22E-04	1.68E-01	-5.55E-05	1.34E-05	1.19E-05
550	155	-3.43E-03	3.48E-01	3.29E-01	-3.11E-04	1.71E-01	-1.46E-05	1.42E-05	1.26E-05
550.00L	155	-3.43E-03	-7.99E-04	-8.57E-04	-2.96E-04	1.71E-01	-5.78E-05	1.42E-05	1.26E-05

Vertical strain in micron = 57.8 x 10^{-06}

Table 5.4: The output result from IITPAVE in Case 3 for rutting of CBR=5%

No. of layers		3							
E values (MPa)		1700.00	16484.86	49.30					
Mu values		0.35	0.35	0.35					
thicknesses (mm)		200.00	150.00						
single wheel load (N)		20000.00							
tyre pressure (MPa)		0.56							
Dual Wheel									
Z	R	SigmaZ	SigmaT	SigmaR	TaoRZ	DispZ	epZ	epT	epR
200	0	-2.09E-01	-1.53E-01	-1.48E-01	-3.38E-02	3.03E-01	-6.08E-05	-1.62E-05	-1.30E-05
200.00L	0	-2.09E-01	-5.03E-01	-4.64E-01	-3.38E-02	3.03E-01	7.85E-06	-1.62E-05	-1.30E-05
200	155	-1.42E-01	-1.23E-01	-1.24E-01	-1.41E-01	3.06E-01	-3.26E-05	-1.76E-05	-1.86E-05
200.00L	155	-1.42E-01	-5.29E-01	-5.41E-01	-1.41E-01	3.06E-01	1.41E-05	-1.76E-05	-1.86E-05
350	0	-1.01E-02	8.67E-01	7.58E-01	-8.18E-04	3.01E-01	-3.51E-05	3.67E-05	2.78-E05
350.00L	0	-1.01E-02	-2.83E-03	-3.15E-03	-8.18E-04	3.01E-01	-1.62E-04	3.67E-05	2.78-E05
350	155	-1.05E-02	9.19E-01	8.16E-01	-1.31E-03	3.05E-01	-3.75E-05	3.86E-05	3.02E-05
350.00L	155	-1.05E-02	-2.90E-03	-3.21E-03	-1.31E-03	3.05E-01	-1.70E-04	3.86E-05	3.02E-05

Vertical strain in micron = 170 x 10^{-06}

Table 5.5: The output result from IITPAVE in Case 4 for rutting of CBR=5%

No. of layers		3							
E values (MPa)		1700.00	16484.86	49.30					
Mu values		0.35	0.35	0.35					
thicknesses (mm)		200.00	100.00						
single wheel load (N)		20000.00							
tyre pressure (MPa)		0.56							
Dual Wheel									
Z	R	SigmaZ	SigmaT	SigmaR	TaoRZ	DispZ	epZ	epT	epR
200	0	-1.62E-01	-1.13E-01	-1.08E-01	-4.88E-02	3.20E-01	-2.80E-05	-6.38E-06	-4.09E-06
200.00L	0	-1.62E-01	-2.23E-01	-2.06E-01	-4.88E-02	3.20E-01	-4.73E-07	-6.38E-06	-4.09E-06
200	155	-9.70E-02	-8.69E-02	-8.73E-02	-1.73E-01	3.24E-01	-1.20E-05	-7.44E-06	-7.66E-06
200.00L	155	-9.70E-02	-2.42E-01	-2.45E-01	-1.73E-01	3.24E-01	4.46E-06	-7.44E-06	-7.66E-06
300	0	-1.15E-02	9.88E-01	8.51E-01	-9.50E-04	3.18E-01	-3.97E-05	4.21E-05	3.09E-05
300.00L	0	-1.15E-02	-3.24E-03	-3.66E-03	-9.50E-04	3.18E-01	-1.85E-04	4.21E-05	3.09E-05
300	155	-1.20E-02	1.04E+00	8.83E-01	-1.71E-03	3.22E-01	-4.15E-05	4.44E-05	3.18E-05
300.00L	155	-1.20E-02	-3.35E-03	-3.81E-03	-1.71E-03	3.22E-01	-1.93E-04	4.45E-05	3.18E-05

Vertical strain in micron = 193 x 10^{-06}

4.3 Effect of reinforcement on surface deformation of the flexible pavement:

4.3.1 Effect reinforcement on surface deformation at 90% reliability for rutting life:

In order to show the effect of reinforcement on flexible pavement, four different cases are considered. Poisson's ratio in the present case is taken as 0.35, Modulus of resilient for bituminous and subgrade is taken as 3000MPa and 49.30 MPa respectively. While the Modulus of resilient for the granular layer without reinforced with reinforced is taken as 350MPa and16484.86MPa respectively. Results have been computed are shown in figure 4.1-4.4.

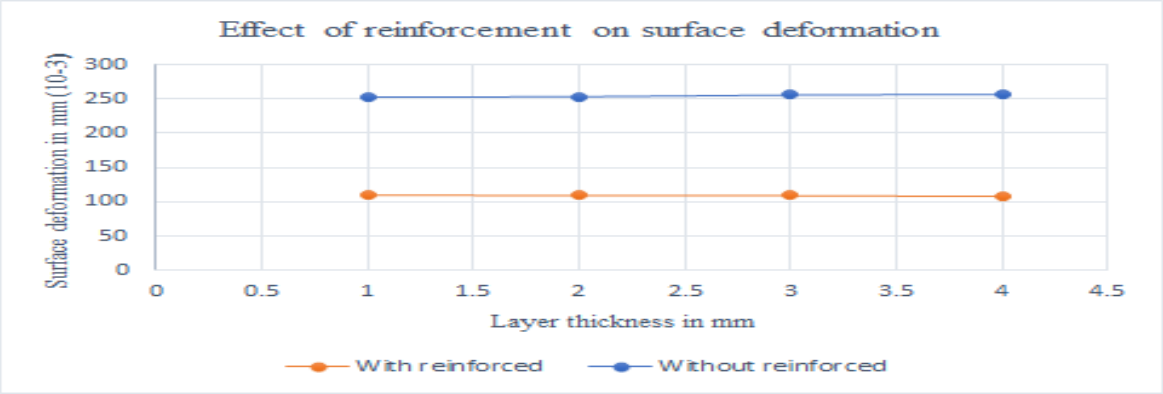

Figure 4.1 Surface deformation for case 1 in rutting life at 90% reliability

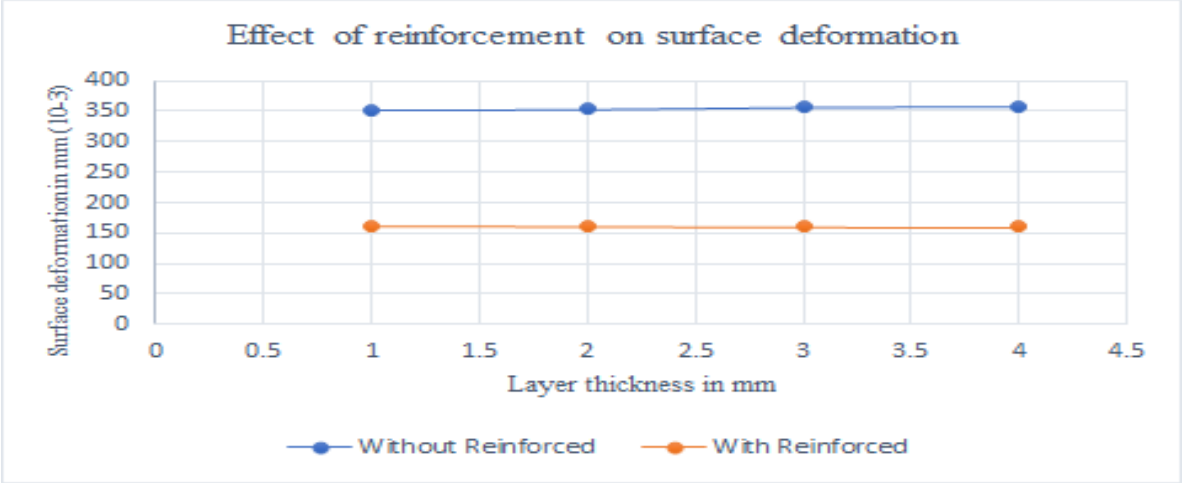

Figure 4.2 Surface deformation for case 2 in rutting life at 90% reliability

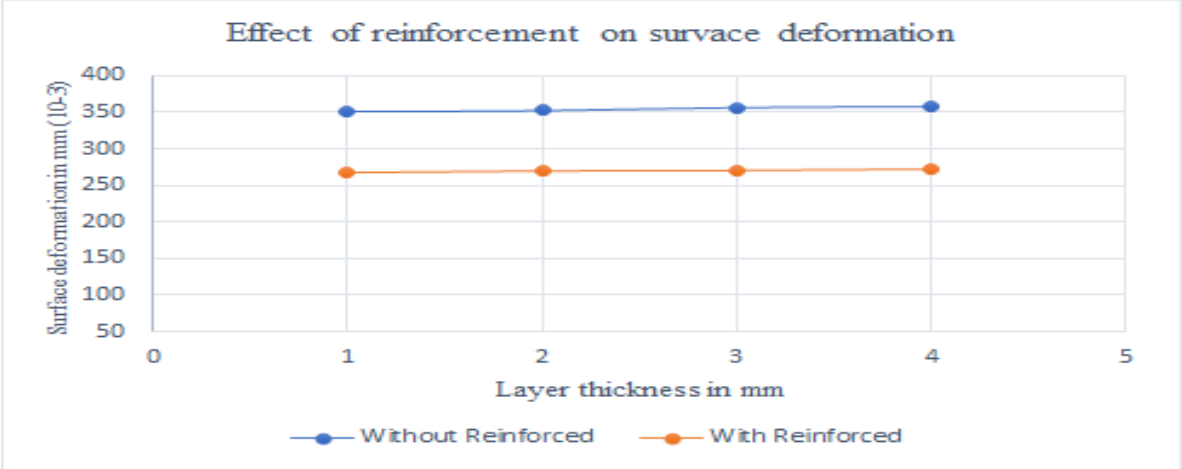

Figure 4.3 Surface deformation for case 3 in rutting life at 90% reliability

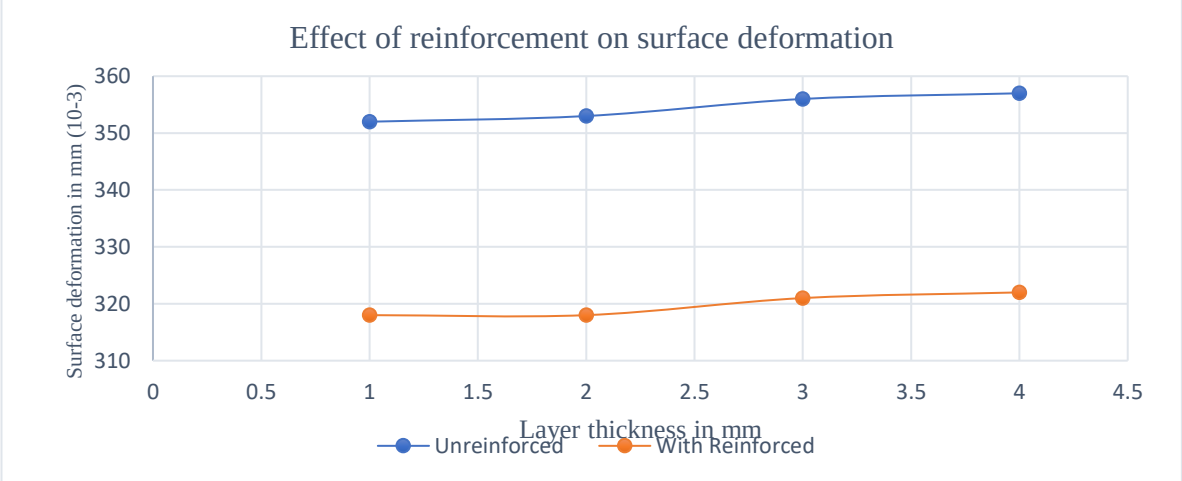

Figure 4.4 Surface deformation for case 4 in rutting life at 90% reliability

From figures 4.1 to 4.4 it can be seen that the reinforcement has a significant influence on surface deformation. It is observed that after all four cases, maximum deformation reduces case4<case3<case2<case1 with respect to unreinforced by 56.91%.

4.3.2 Effect reinforcement on surface deformation at 80% reliability for rutting life:

In order to show the effect of reinforcement on flexible pavement, four different cases are considered. The soil profile for the four cases is kept the same. Poisson's ratio in the present case is taken as 0.35, the thickness of a bituminous layer is taken as 200mm, tyre pressure 0.56 MPa, Single wheel load 20000 N, Modulus of resilient for bituminous and subgrade is taken as 1700 MPa and 49.30 MPa respectively. While the Modulus of resilient for the granular layer without reinforced with reinforced is taken as 350MPa and16484.86MPa respectively. Results have been computed are shown in figure 4.5-4.8.

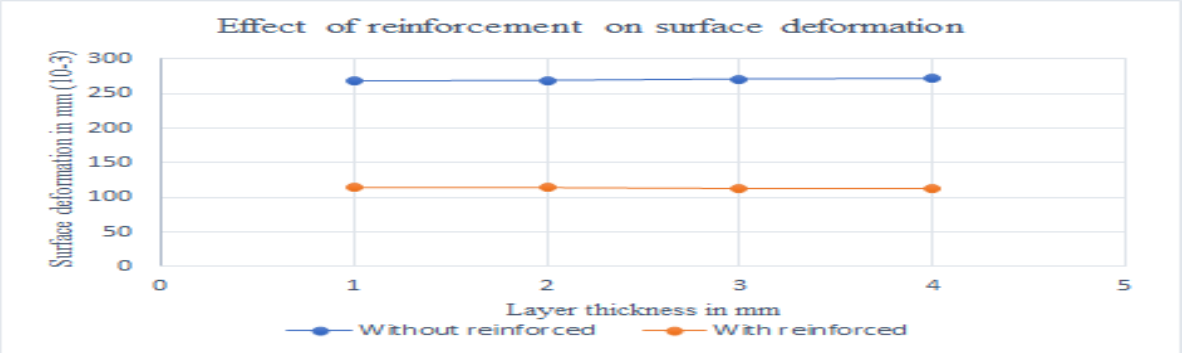

Figure 4.5 Surface deformation for case 1 in rutting life at 80% reliability

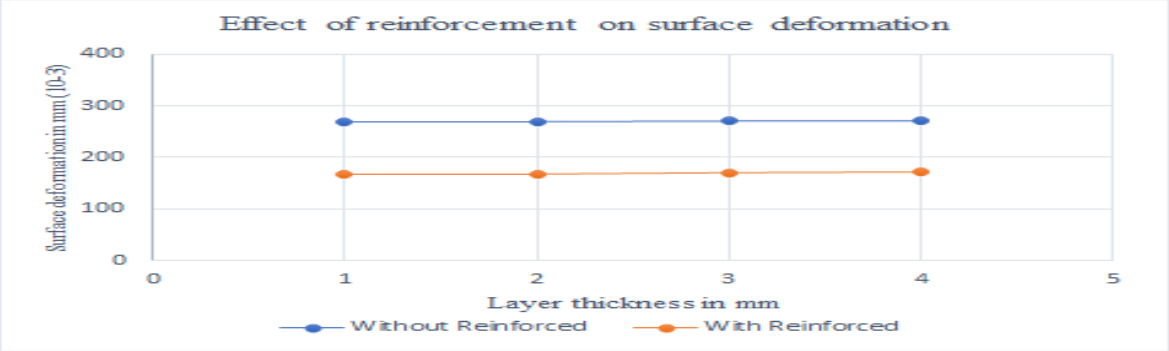

Figure 4.6 Surface deformation for case 2 in rutting life at 80% reliability

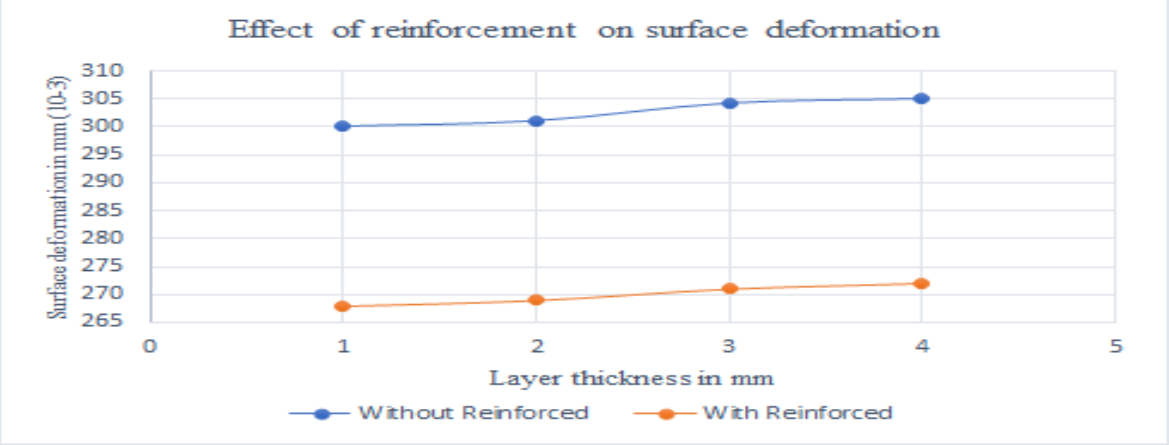

Figure 4.7 Surface deformation for case 3 in rutting life at 80% reliability

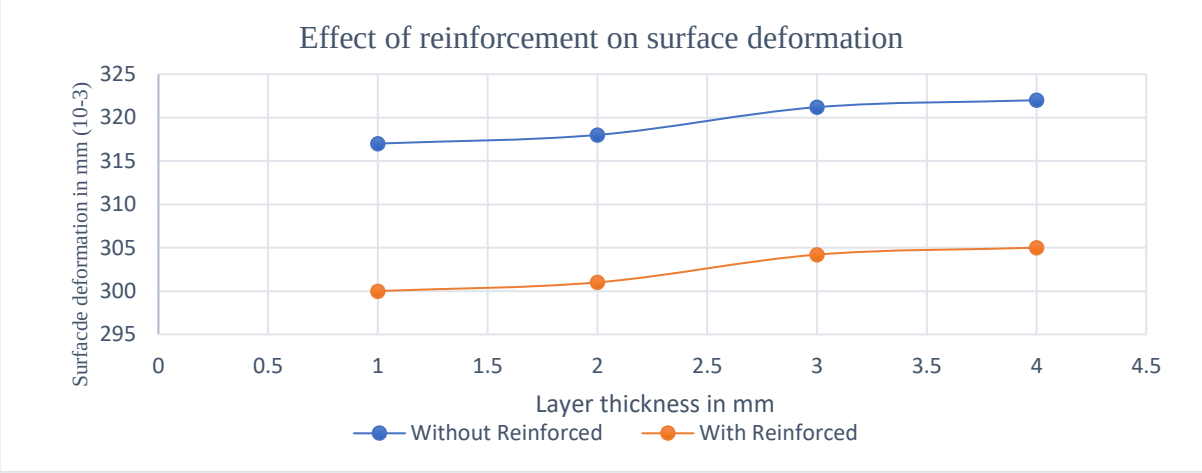

Figure 4.8 Surface deformation for case 4 in rutting life at 80% reliability

For 100 MSA traffic, from figure 4.5 -figure 4.4 it can be seen that the reinforcement has a significant influence on surface deformation. For all four cases, maximum deformation reduces case4<case3<case2<case1 with respect to unreinforced by 57.83%.

4.4 Effect of reinforcement on a tangential strain of the flexible pavement:

4.4.1 Effect reinforcement on tangential strain at 90% reliability for 100 MSA traffic:

In order to show the effect of reinforcement on tangential strain in the flexible pavement, four cases are considered. Poisson's ratio in the present case is taken as 0.35, the thickness of a bituminous layer is taken as 200mm, tyre pressure 0.56 MPa, Single wheel load 20000 N, Modulus of resilient for bituminous and subgrade is taken as 3000 MPa and 49.30 MPa respectively. While the Modulus of resilient for a granular layer with reinforced is taken as 16484.86MPa. Results have been computed at two radial distances of '0' and '155' as shown in figure 4.9-figure 4.12.

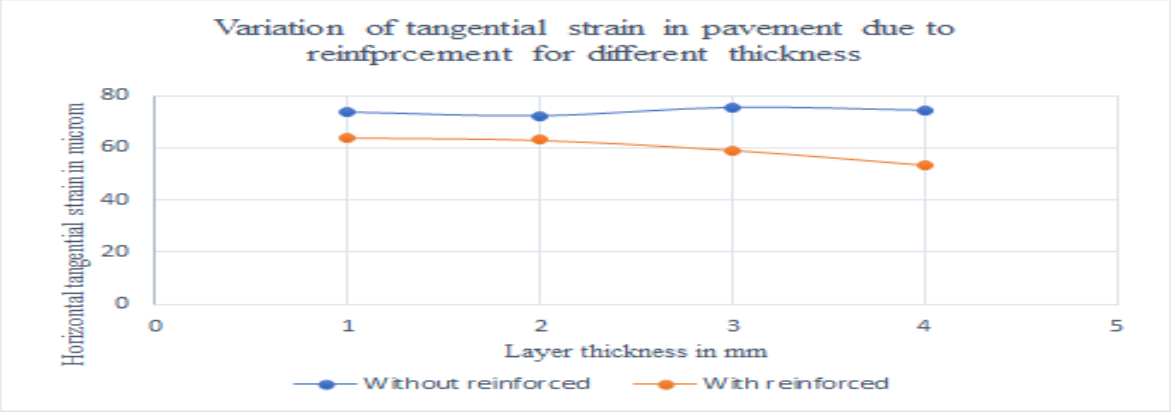

Figure 4.9 Variation of tangential strain for case 1 in rutting life at 90% reliability

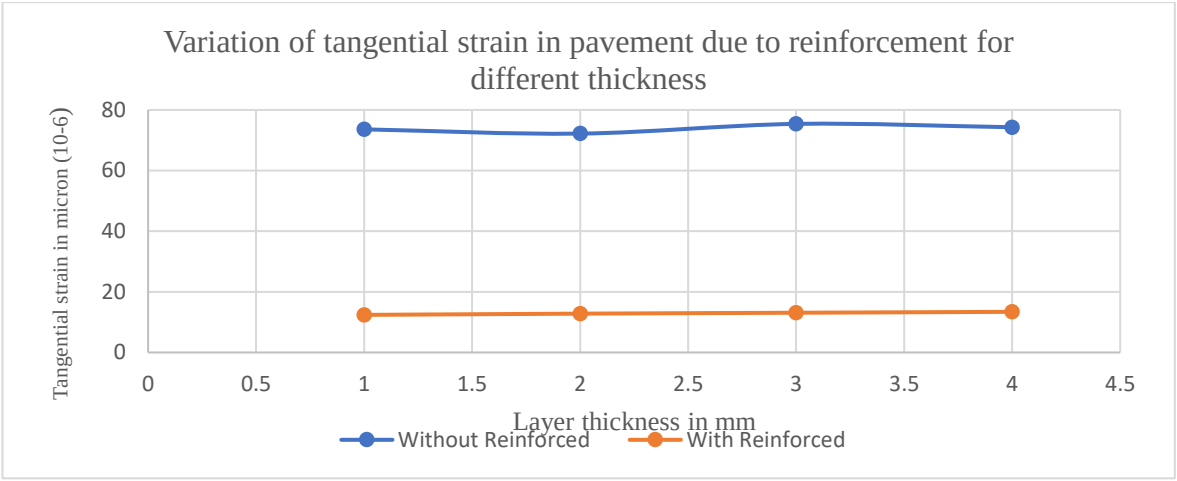

Figure 4.10 Variation of tangential strain for case 2 in rutting life at 90% reliability

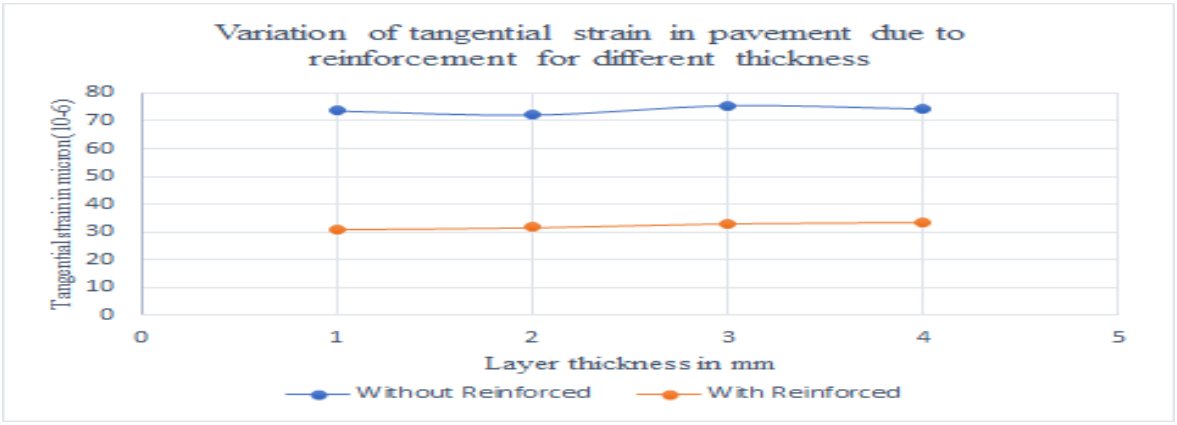

Figure 4.11 Variation of tangential strain for case 3 in rutting life at 90% reliability

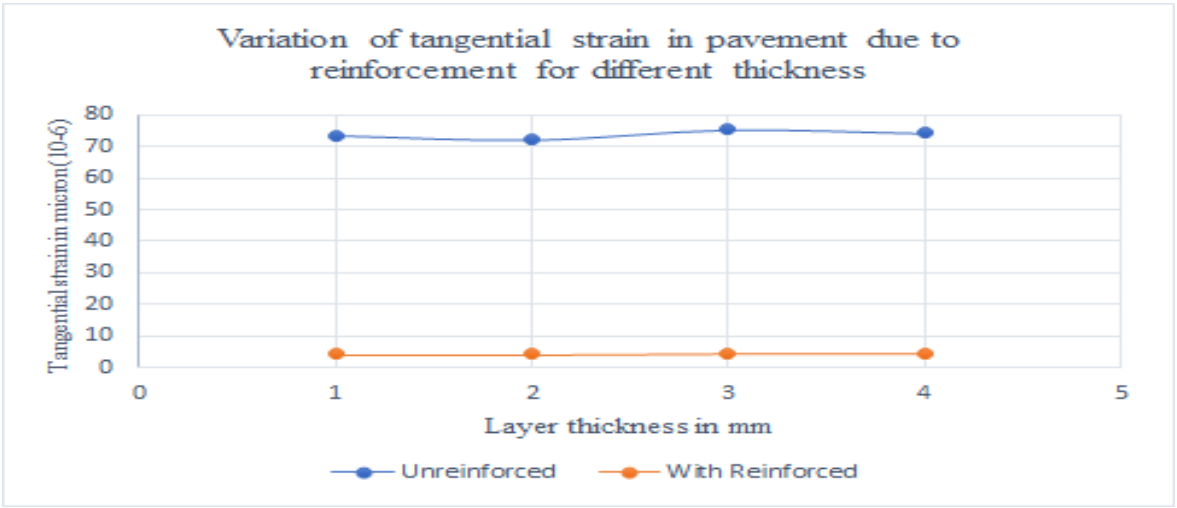

Figure 4.12 Variation of tangential strain for case 4 in rutting life at 90% reliability

For 100 MSA traffic, from figure 4.9 -figure 4.12 it can be seen that the reinforcement has a significant reduction in tangential strain. It is observed that the maximum reduction of tangential strain with respect to unreinforced by 39.67%. It is also observed that the maximum tangential strain is less than the allowable strain of the pavement.

4.4.2 Effect reinforcement on tangential strain at 80% reliability for rutting life:

The effect of reinforcement on tangential strain in the flexible pavement, four cases are considered. Poisson's ratio is taken as 0.35 for all layers, the thickness of a bituminous layer is taken as 200mm, tyre pressure 0.56 MPa, Single wheel load 20000 N, Modulus of resilient for bituminous and subgrade is taken as 1700 MPa and 49.30 MPa respectively. While the Modulus of resilient for a granular layer with reinforced is taken as 16484.86MPa. Results have been computed at two radial distances of '0' and '155' as shown in figure 4.13-figure 4.16.

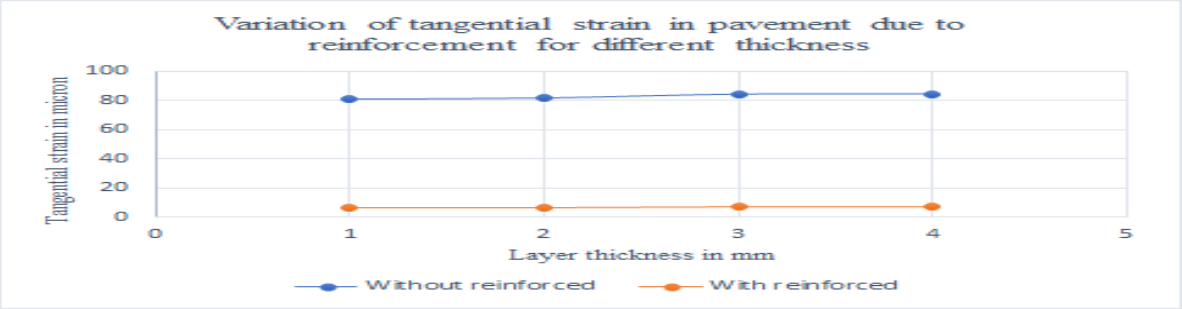

Figure 4.13 Variation of tangential strain for case 1 in rutting life at 80% reliability

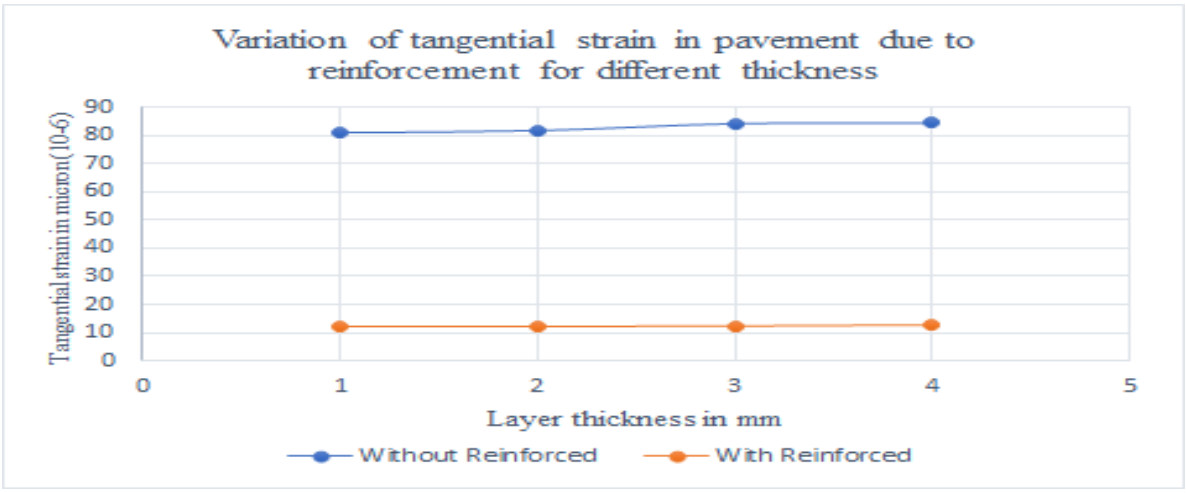

Figure 4.14 Variation of tangential strain for case 2 in rutting life at 80% reliability

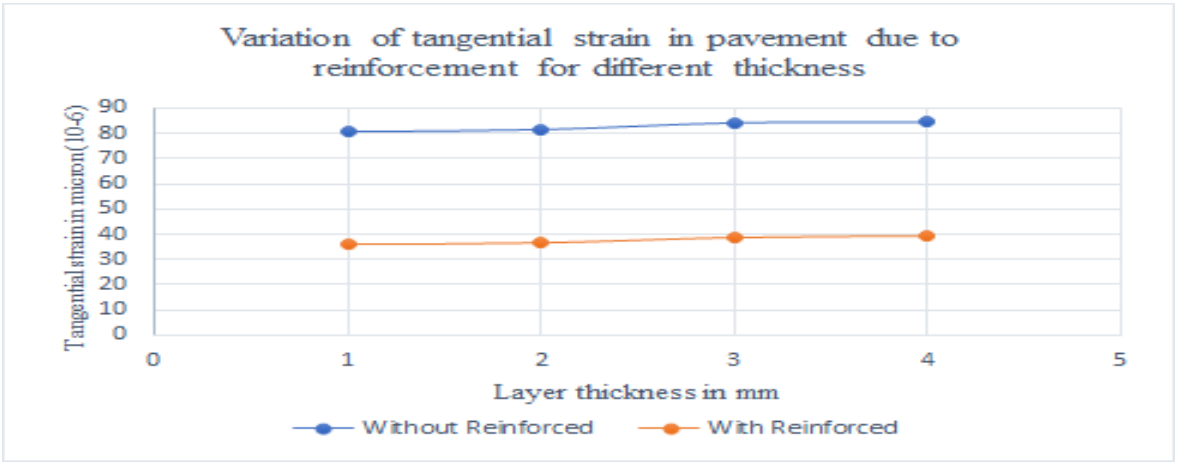

Figure 4.15 Variation of tangential strain for case 3 in rutting life at 80% reliability

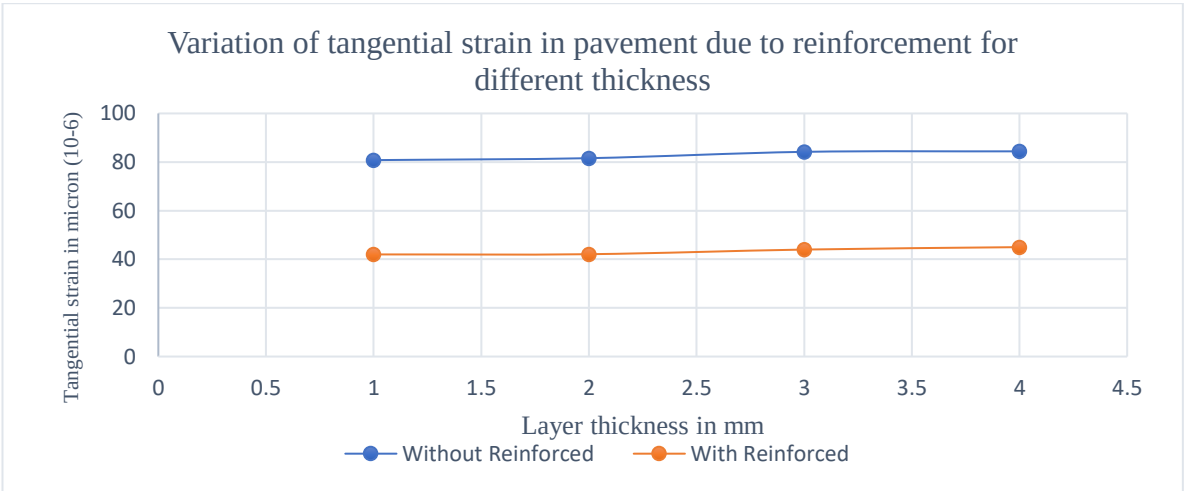

Figure 4.16 Variation of tangential strain for case 4 in rutting life at 80% reliability

From figure 4.13 -figure 4.16, For 100 MSA traffic, it can be seen that the reinforcement has a significant reduction in tangential strain. It is observed that the maximum reduction of tangential strain with respect to unreinforced by 47.15%. It is also observed a similar nature is found for all four cases and the maximum actual strain found is 169 microns which are less than the permissible strain.

4.5 Effect of reinforcement on a radial strain of the flexible pavement:

4.5.1 Effect reinforcement on radial strain at 90% reliability for rutting life:

For the effect of reinforcement on radial strain in the flexible pavement, four cases are considered Poisson's ratio taken as 0.35 for all layers, the thickness of a bituminous layer is taken as 200mm, tyre pressure 0.56 MPa, Single wheel load 20 KN, Modulus of resilient for bituminous and subgrade is taken as 3000 MPa and 49.30 MPa respectively. While the Modulus of resilience for a granular layer with reinforced and without reinforcement is taken as 16484.86MPa 350MPa respectively. Results have been computed at two radial distances of '0' and '155' as shown in figure 4.13-figure 4.20.

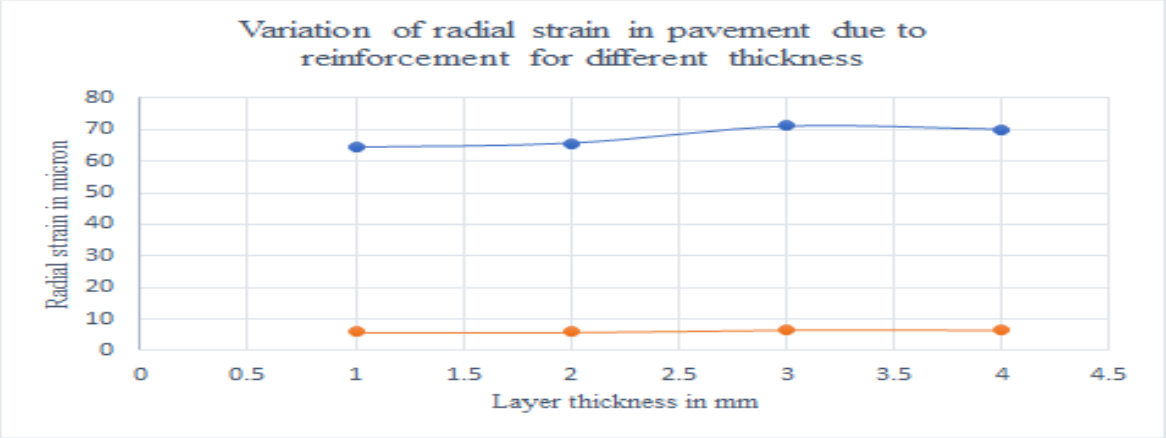

Figure 4.17 Variation of radial strain for case 1 in rutting life at 90% reliability

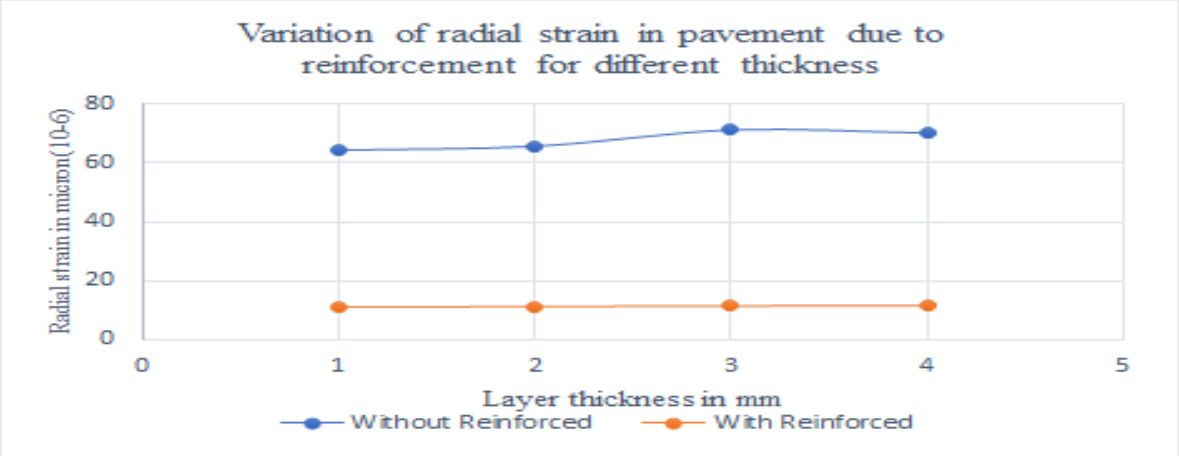

Figure 4.18 Variation of radial strain for case 2 in rutting life at 90% reliability

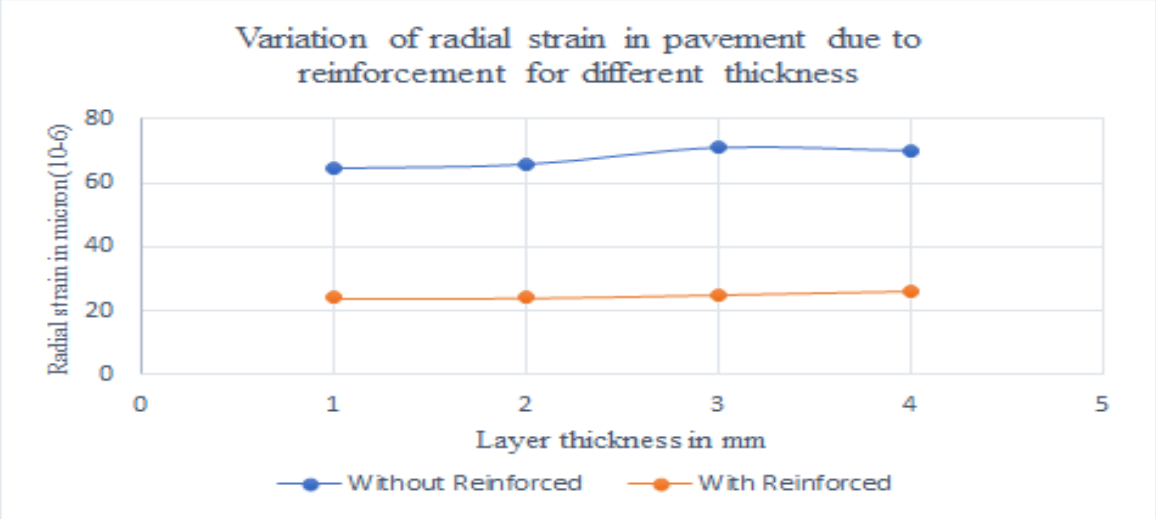

Fig.4.19 Variation of radial strain for case 3 in rutting life at 90% reliability

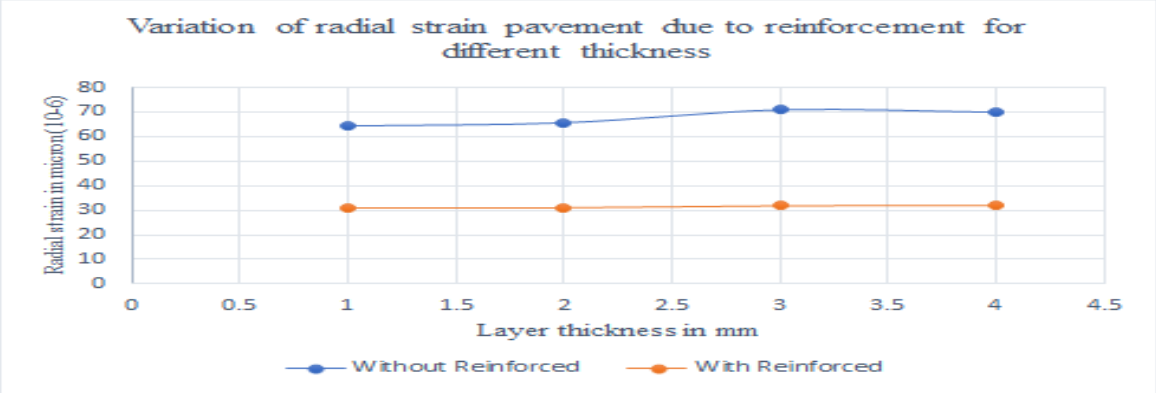

Fig.4.20 Variation of radial strain for case 4 in rutting life at 90% reliability

Figure 4.17-4.12 Variation of radial strain with respect to different layer thickness for different cases.

The above Figure reveals that initially radial strain decreases then increases with a decrease in the thickness of a base layer of reinforced pavement. it can be seen that the reinforcement has a reduction in radial strain with respect to unreinforced by54.63%. It is also observed a similar nature is found for all four cases and the maximum actual strain is less than the permissible strain.

4.5.2 Effect reinforcement on radial strain at 80% reliability for rutting life:

The effect of reinforcement on radial strain in the flexible pavement, four cases different are case1 case2 case3 case4 considered. Poisson's ratio is taken as 0.35 for all layers, the thickness of a bituminous layer is taken as 200mm, tyre pressure 0.56 MPa, Single wheel load 20 KN, Modulus of resilient for bituminous and subgrade is taken as 1700 MPa and 49.30 MPa respectively. While the Modulus of resilient for a granular layer with reinforced and without reinforcement is taken

as 16484.86MPa 350MPa respectively. Results have been computed at two radial distances of '0' and '155' as shown in figure 4.21-figure 4.24.

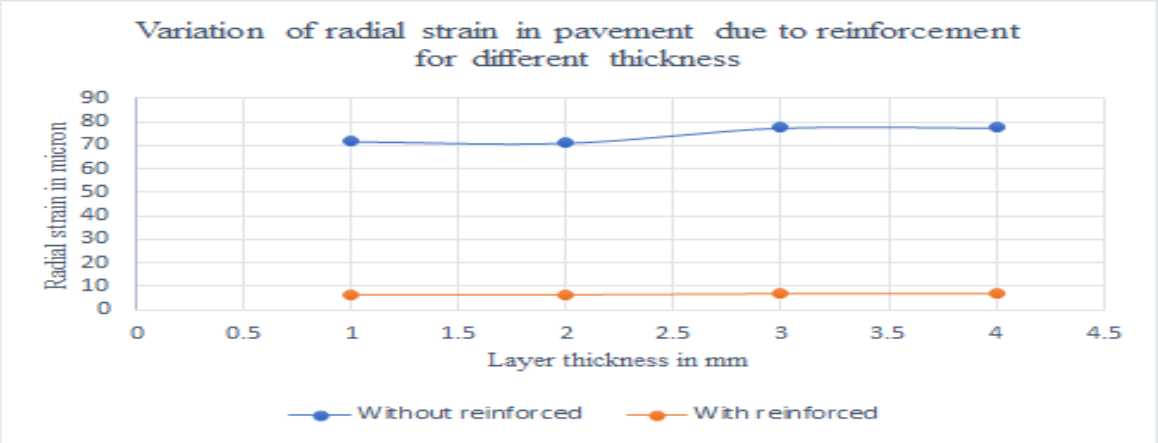

Fig.4.21 Variation of radial strain for case 1 in rutting life at 80% reliability

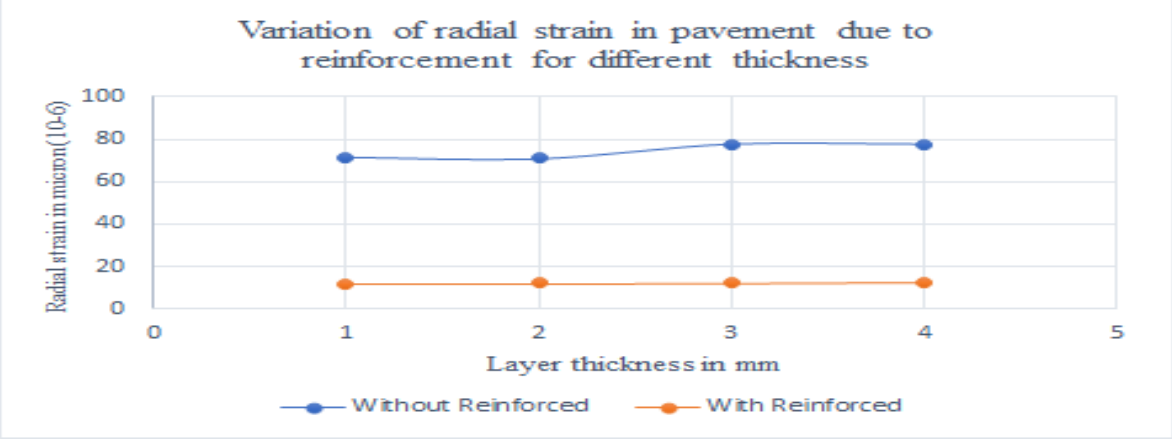

Fig.4.22 Variation of radial strain for case 2 in rutting life at 80% reliability

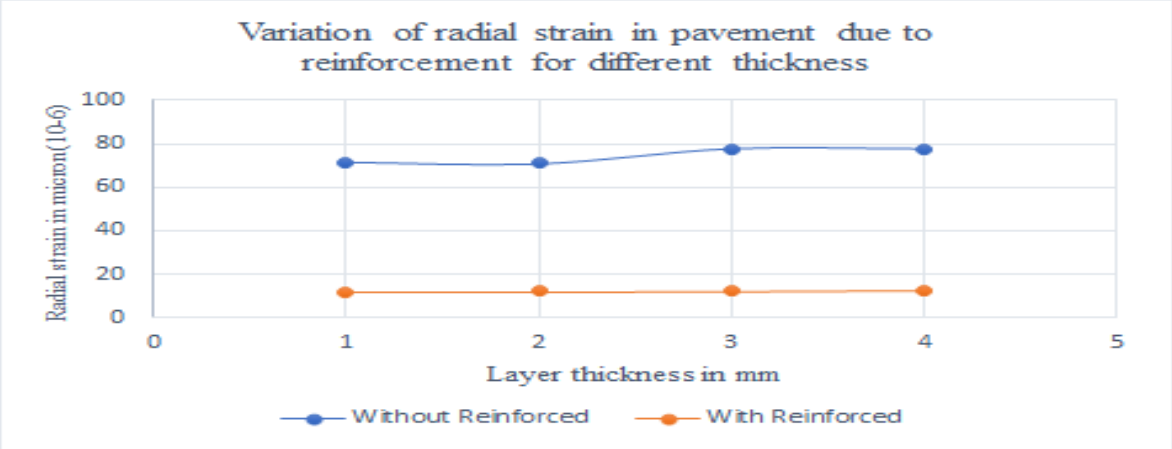

Fig.4.23 Variation of radial strain for case 3 in rutting life at 80% reliability

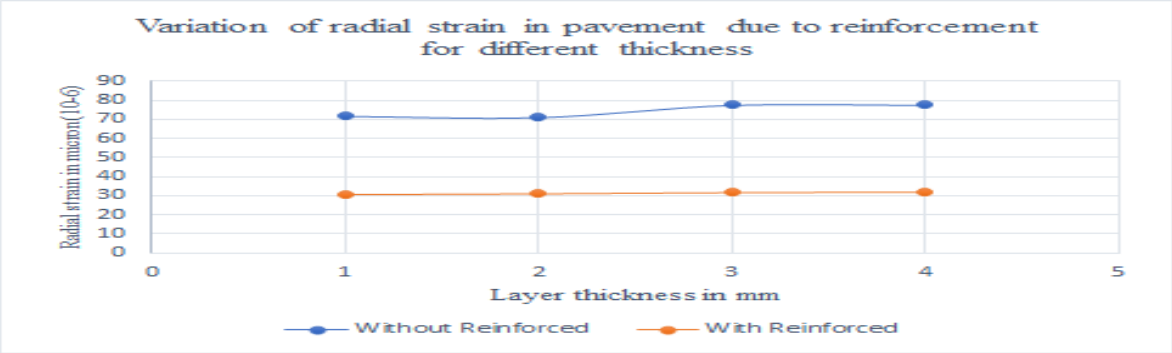

Fig.4.24 Variation of radial strain for case 4 in rutting life at 80% reliability

For 100 MSA traffic, from figure 4.21 -figure 4.24 it can be seen that the reinforcement has a. It is observed that the maximum reduction of tangential strain with respect to unreinforced by 51.24%. It is also observed that the maximum tangential strain is less than the allowable strain of the pavement.

4.6 Table 4.6.1: Pavement Composition of soil with geo-reinforcement (geogrid) for Rutting life and Fatigue life 100 MSA:

Sl.no	CBR	Granular layer thickness (mm)	DBM (mm)	BC (mm)	Total thickness (mm)	Actual ε_z*	Actual ε_t*1	Allowable ε_z**	Allowable ε_t**2	Rutting life (MSA)	% saving in granular layer thickness	% saving in overall layer thickness
1	5	550	150	50	750	191.0	141	319	170	100	0	0
2	5	550	150	50	750	26.11	143	319	170	100	0	0
3	5	350	150	50	550	57.70	1162	319	170	100	36.36	26.66
4	5	150	150	50	350	141.0	168	319	170	100	72.72	80.00
5	5	100	150	50	300	187.0	169.2	319	170	100	81.81	86.66

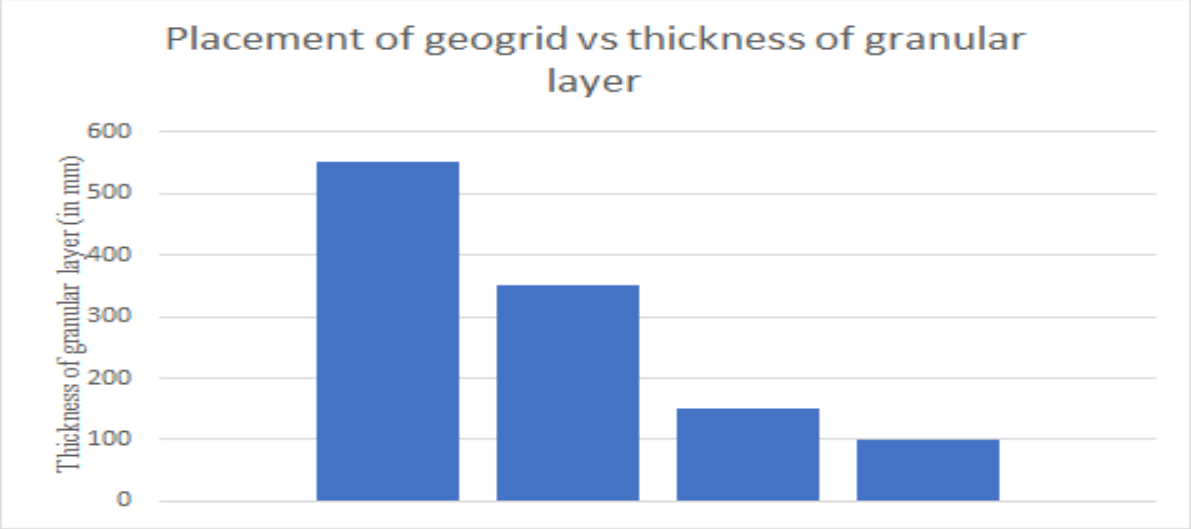

Fig.4.25 Placement of geogrid vs thickness of a granular layer

In fatigue life analysis, the thickness of the granular subbase layer and granular base (wet mix macadam) layer is constant (300+250 = 550 mm), such that the dense bituminous macadam (DBM) layer's thickness is reduced and then the reinforcement (geogrid) is placed in different locations. The critical horizontal strain is calculated from IITPAVE software. For fatigue life 100 MSA, this critical strain value should be less than the allowable horizontal strain value calculated (as equations 5.1 and 5.2).

In rutting life analysis, the thickness of the dense bituminous macadam layer and a bituminous concrete layer is constant (150+50 = 200 mm) so that the thickness of the granular layer is decreased followed by the geo-reinforced (geogrid) placed at different locations. The critical vertical strain is calculated from IITPAVE software. For rutting life 100 MSA, this critical strain value should be less than the allowable vertical strain value calculated (as equations 5.3 and 5.4). The percentage saving of granular layer thickness is also computed. Table 5.1 represent the Pavement Composition with geo-reinforced (geogrid) at a different location and their output results from IITPAVE, in Rutting Life 100MSA at 90% and 80% reliability.

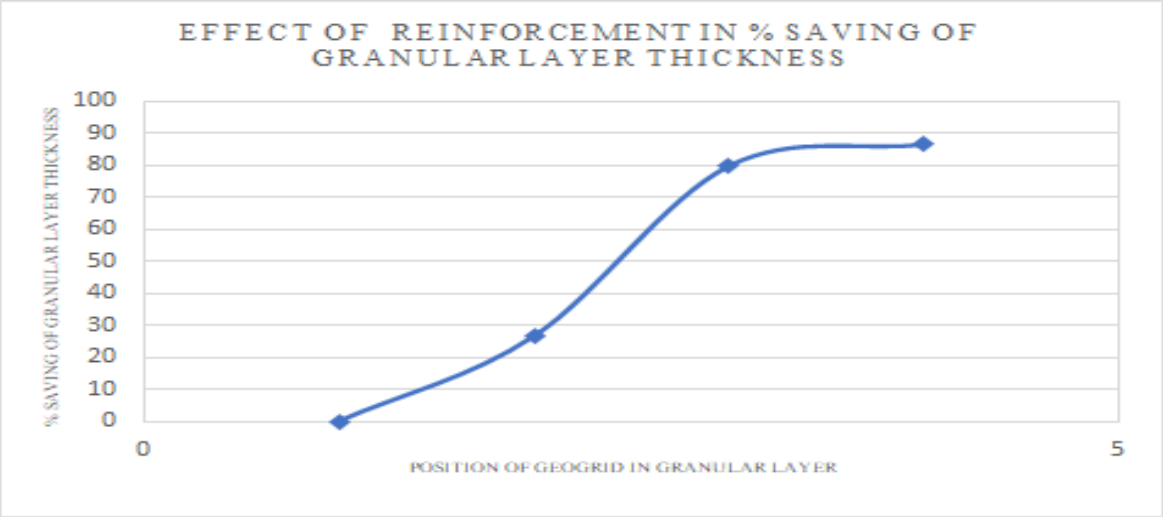

Figure 4.26 Effect of reinforcement in % saving of granular layer

For Traffic life 100 MSA and California bearing ratio (CBR) of 5%, when the geogrid is placed at different depths in granular layer i.e. 550mm, 350mm, 150mm, 100mm; there is a saving of thickness of granular layer are 26.66%, 80% and 86.66% at 90% reliability as shown in figure 4.26 and figure 4.25 gives the variation of granular thickness in the pavement.

4.7 Cost Analysis:

A detailed cost analysis has been carried out for the unreinforced and geogrid reinforced pavement sections. The cost of the granular base and bituminous layer is taken from the PWD of GOI. The cost analysis is carried out of a dual carriageway flexible pavement and the results are tabulated in Tables 4.7.2 and 4.7.5 respectively. It can be seen that a net savings of Rs. 1,18,23,750 can be accounted for a km of reinforced flexible pavement section than the unreinforced pavement section. A reduction of about 38.08% was observed in the construction cost of a km stretch of flexible pavement.

Table 4.7.2 Cost analysis of a km stretch of unreinforced flexible pavement (Case 1)

Sl. No.	Description	Layers	Length (m)	Width (m)	Layer thickness (mm)	Cost of layer/m^3 (Rs)	The total cost of Layer/Km (Rs)
1	Soil without reinforcement CBR=5% for traffic =100MSA	GSB	1000	7.5	300	3570	80,32,500
2		GB(WMM)	1000	7.5	250	3720	69,75,000
3		DBM	1000	7.5	150	10235	1,15,14,375
4		BC	1000	7.5	50	12065	45,24,375
5		**Total Cost of Pavement per Km (Rs)**					3,10,46,250

Table 4.7.3 Cost analysis of a km stretch of reinforced (geogrid) flexible pavement (Case 2)

Sl. No.	Description	Layers	Length (m)	Width (m)	Layer thickness (mm)	Cost of layer/m^3 (Rs)	The total cost of Layer/Km (Rs)
1		GSB	1000	7.5	200	3570	53,55,000

2	Soil without reinforcement CBR=5% for traffic =100MSA	WMM	1000	7.5	150	3720	41,85,000
3		DBM	1000	7.5	150	10235	1,15,14,375
4		BC	1000	7.5	50	12065	45,24,375
5		Cost for Geogrid and its laying @60/ sq. mt					4,50,000
6		**Total Cost of Pavement per Km (Rs)**					2,60,28,750

Table 4.7.4 Cost analysis of a km stretch of reinforced (geogrid) flexible pavement (Case 3)

Sl. No.	Description	Layers	Length (m)	Width (m)	Layer thickness (mm)	Cost of layer/m^3 (Rs)	The total cost of Layer/Km (Rs)
1	Soil without reinforcement CBR=5% for traffic=100MSA	GSB	1000	7.5	150	3570	40,16,250
2		WMM	1000	7.5	150	3720	41,85,000
3		DBM	1000	7.5	150	10235	1,15,14,375
4		BC	1000	7.5	50	12065	45,24,375
5		Cost for Geogrid and its laying @60/ sq. mt					4,50,000
6		**Total Cost of Pavement per Km (Rs)**					2,46,90,000

Table 4.7.5 Cost analysis of a km stretch of reinforced (geogrid) flexible pavement (Case 4)

Sl. No.	Description	Layers	Length (m)	Width (m)	Layer thickness (mm)	Cost of layer/m^3 (Rs)	The total cost of Layer/Km (Rs)
1	Soil with reinforcement CBR=5% for traffic=100MSA	GSB+WMM	1000	7.5	100	3645	27,33,750
2		DBM	1000	7.5	150	10235	1,15,14,375
3		BC	1000	7.5	50	12065	45,24,375
4		Cost for Geogrid and its laying @60/ sq. mt					4,50,000
5		**Total Cost of Pavement per Km (Rs)**					1,92,22,500

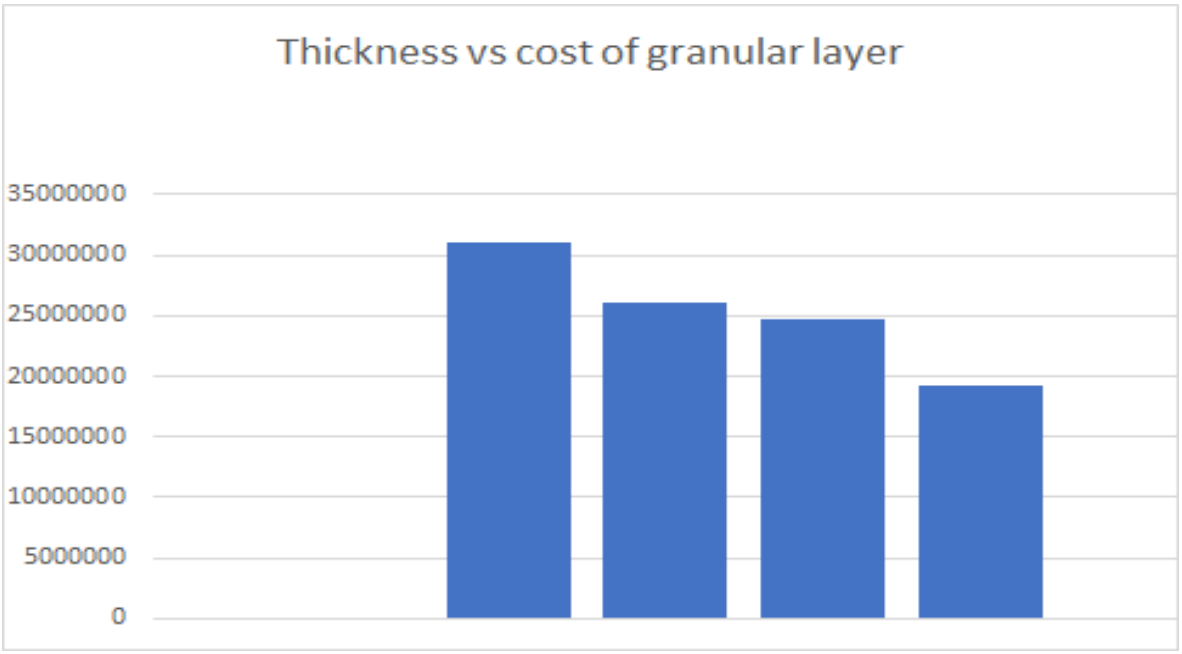

Fig.4.27 Comparison of different cases of granular layer vs cost

Figure 4.27 reveals that comparison of different cases of a granular layer with respect to cost. Provides an economical solution saving the natural resources used in pavement construction. It is found that reinforced pavement costs approximately 40% cheaper than unreinforced pavement

Chapter 5

CONCLUSIONS AND FUTURE SCOPE OF THE STUDY

This chapter presents the summary of the study conducted, conclusions that can be drawn from the study and limitations of the study presented. Further, future scopes of the study are also presented to conclude the thesis.

5.1 Conclusions

This study proposed a mechanistic-empirical method to measure the effect of geosynthetics on the performance of the flexible pavement. The following major conclusions can be drawn from the study performed.

- The use of geosynthetics can reduce pavement thickness, and thus, can save natural resources in a significant manner. It is noticed that by inserting geogrid into the granular base layer, the base thickness can be reduced by 87% compared to the unreinforced section compared to a similar performance level observed for the case of the unreinforced section. For example, the geogrid-reinforced pavement section with a reduced thickness (100 mm base thickness) performs better than the unreinforced pavement section with a base thickness 550 mm in all respects.
- The geogrid helps in decreasing the permanent deformations of the pavement by enhancing the elasticity of the respective layers. In the reinforced case, there has been a 57% decrease in total observed permanent deformation.
- In comparison to the unreinforced pavement, the geogrid reinforced granular base layer has experienced a significant reduction in the tensile strain. Reduction in vertical compressive stresses under the wheel was also observed to be significantly reduced due to modifications made with geogrid.
- The conclusions of the numerical analysis show that the resilient modulus of the pavement granular base layer was improved due to the inclusion of geogrid in the granular base layer as compared to unreinforced pavement.
- Cost is the single most important consideration for any civil engineering project. After comparing the cost analysis, it's clear that for every km of

single-lane road construction, reinforced pavement costs 38.08% cheaper than unreinforced pavement.

5.2 Scope for the Future Study

The scope of application of geo-reinforcement to the unpaved road in geotechnical engineering problems is very significant. Some recommendations for further research are made as follows:

- This present study is mainly done on the strength criteria of the pavement such as rutting and fatigue failure criteria. However, the functional criteria where defects occur have not been considered which may be addressed as future scope of the study.
- The study has only considered the geogrid as the reinforcement; whereas, at present geocell and other combinations of geosynthetics are getting popularity. Hence, in future, this scope can also be explored.
- The numerical study couldn't be verified with real-time data and/or physical model tests. This may be addressed in future to conclude the advantage of the use of geosynthetics in pavement sub-structure.

REFERENCES

[1] “Guidelines for the design of flexible pavements” IRC:37-2018 (Fourth Revision).

[2] Indian Road Congress, (2012). Guidelines for the design of flexible pavements. Indian code of practice, IRC-37, New Delhi.

[3] Alavi, A. H., Aminian, P., Gandomi, A. H., and Esmaeili, M. A., (2011). "Genetic-based modeling of uplift capacity of suction caissons". *Expert Systems with Applications*, 38, 12608- 12618.

[4] Alavi, A. H., and Gandomi, A. H., (2012). "Energy-based numerical models for assessment of soil liquefaction". *Geoscience Frontiers*, 3(4), 541-555.

[5] Benjamin, C.V.S., Bueno, B., and Zornberg, J.G., (2007). "Field monitoring evaluation of geotextile-reinforced soil retaining walls". *Geosynthetics International Journal*, Vol.14, No. 1.

[6] Shin, E.C., Kim, D.H., and Das, B.M., 2002. "Geogrid reinforced rail road bed settlement due to cyclic load". *Geotechnical and Geological Engineering*, Vol. 20, No. 3, 261-271.

[7] Mehdipour Iman., Ghazavi. Mahmoud., and Moayed Ziaie Reza., (2013)." Numerical study on stability analysis of geocell reinforced slopes by considering the bending effect". *Geotextiles and Geomembranes*, 37(2013), 23-34.

[8] https://www.aboutcivil.org/flexible-pavement-road.html

[9] https://www.aboutcivil.org/flexible-pavement-road.html

[10] Guidelines for use of geosynthetics in road pavements and associated works (first revision):IRC:SP:59-2019

[11] Geofoam Market 05-12-2020 08:30 AM CET Industry, Real Estate & Construction Press release from: Premium Market Insights

[12] “Usage of geogrid in flexible pavement design”-Peketi Madhu Ganesh Yadav*1, Singalareddy Bharath2, Mekala Manoj Kumar3, Mallem Niranjan Reddy4 & Gadikota ChennaKesava Reddy5

[13] “Effect of the position of geotextile on the strength characteristics of the subgrade in bituminous pavement”-Tarun gupta, Rajesh Pathak and Tanuj Chopra`

[14] Al-Qadi I., Dessouky S., Kwon J., and Tutumluer E., (2008). “Geogrid in flexible pavements: Validated mechanism” *Transportation Research Record 2045, Transportation Research Board*, Washington, DC, 102–109.

[15] Liu Chia-Nan., Yang Kuo-Hsin., and Nguyen Duc Minh., (2014). “Behavior of geogrid reinforced sand and effect of reinforcement anchorage in large scale plane strain compression”. *Geotextiles and Geomembranes*, 42(2014), 479 - 493.

[16] S. A. Naeini and R. Ziaie Moayed (2009), “Effect of plasticity index and reinforcement on the CBR value of soft clay”.

[17] Huang, C.C., and Menq, F.Y., (1997). “Deep footing and wide-slab effects on reinforced sandy ground”.

[18] Dr. D. S. V. Prasad and Dr M. Anjan Kumar (2010), “Behaviour of reinforced sub bases on expansive soil sub-grade”.

[19]
Sivapragasam, C, Vanitha, S, V. M. Arun and S. Sutharsanam (2010), " Study on Synthetic Geotextiles for Road Pavements".

[20] A. K. Choudhary, K.S. Gill and J.N. Jha (2011), “Improvement in CBR values of
expansive soil sub-grades using geo-synthetics”.

[21] Pardeep Singh, K.S. Gill (2012), “CBR Improvement of clayey soil with geo-grid

reinforcement".

[22] Sarika B. Dhule, S.S. Valunjkar, and S.D. Sarkate (2011), "Improvement of Flexible Pavement with Use of Geogrid".

[23] Dr. P. Senthil Kumar, and R. Rajkumar (2012), Effect of Geotextile on CBR
Strength of Unpaved Road with Soft Sub grade.

[24] Gu Jie., (2011). "Computational Modeling of Geogrid Reinforced Soil Foundation and Geogrid Reinforced Base in Flexible Pavement". *Ph.D. dissertation*. Louisiana State Univ., Baton Rouge, LA.

[25] Palmeira Marques Ennio., (2009). "Soil–geosynthetic interaction: Modelling and analysis".

[26] Perkins, S.W., (2001). "Mechanistic empirical modelling and design model development of geosynthetics reinforced flexible pavements",

[27] S. K. Ahirwar and J. N. Mandal. (2017), "Finite Element Analysis of Flexible Pavement with geogrids".

[28] Adel A. Al-Azzawi. (2012). "Finite element analysis of flexible pavements strengthend with geogrid**"** *ARPN Journal of Engineering and Applied Sciences,* Volume-7, 1295-1299.

[29] "Strength characteristics of reinforced soil" M.R.Hausmann, LK.Lee (1976).

[30] Zoenberg, J.G., (2012). "Geosynthetic reinforced pavement system". *5th European Geosynthetic Congress. Valencia,* (2012). 49-61.

[31] AASHTO M145 (2012) AASHTO soil classification systems. Standard specifications for transportation materials and methods of sampling and testing. AASHTO, Washington, DC

[32] AASHTO T11 (2012) Materials finer than 75-lm (no. 200) sieve in mineral aggregates by washing. Standard specifications for transportation materials and methods of sampling and testing. AASHTO, Washington, DC

[33] Bush D.I., Jenner C.G. and Besset R.H. The design and construction of geocell foundation mattress supporting over soft grounds, Geo-textiles and Geomembranes, Vol. 9, (1990) 83-98.

[34] Barksdale, R. D., Brown, S. F., & Chan, F. (1989) Potential benefits of geo-synthetics in flexible pavement systems (No. 315).